Doctoral Dissertation

Non-Linear Analysis of Frictional Interface of Hydrogels

（ハイドロゲルの摩擦界面における非線形解析）

Satoshi Hirayama

Graduate School of Life Science, Hokkaido University

2020. 9

Table of Contents

Chapter 1. General Introduction ……... 1

References ……...4

Chapter 2. Non-Linear Analysis of Frictional Interface of Gel in Water ……6

2.1. Introduction ……. 6

2.2. Experiment …….. 6

2.2.1. Materials ……..… 6

2.2.2. Preparation of hydrogels ……..…… 7

2.2.3. Frictional substrate ……..……... 7

2.2.4. Compression test …… 8

2.2.5. Viscosity measurement ……... 8

2.2.6. Dynamic viscoelasticity measurement ……..…. 8

2.2.7. Strain sweep test ……..8

2.2.8. Oscillatory test for Lissajous curves ……...10

2.2.9. *In situ* observation system for frictional interface …… ….10

2.3. Results and Discussion ……...… 11

2.3.1. Dynamic viscoelasticity of PVA gel ……..….. ….11

2.3.2. Strain sweep test ……....11

2.3.3. Lissajous curves ….……..…….…… 11

2.3.4. Two dimensionless parameters for analysis of Lissajous curves …...14

2.4. Conclusion ……..… 18

References …… 19

Figures …….. 21

Chapter 3. Non-Linear Analysis of Frictional Interface of Gel in Concentrated HA Solution ……... 39

3.1. Introduction ……... 39

3.2. Experiments ……...… 39

3.2.1. Materials ……...…… 39

3.2.2. Hydrogels …..……... 39

3.2.3. HA solution ……..…….…… 39

3.2.4. Viscosity measurement ……..…40

3.2.5. Dynamic viscoelasticity measurement ……..…… 40

3.2.6. Strain sweep test ……..…….…… 40

3.2.7. Oscillatory test for Lissajous curves …….…… 40

3.3. Results and Discussion …….. 40

3.3.1. Rheological properties of concentrated HA solution …… 41

3.3.2. Strain sweep test……....…… 41

3.3.3. Lissajous curves ……...…… 42

3.3.4. Two dimensionless parameters for analysis of Lissajous curves …. 42

3.4. Conclusion ……...…….. 44

References …… 45

Figures …….. 46

Chapter 4. Contact Pattern Formation by Oscillatory Shearing ……..… 54

4.1. Introduction ……... 54

4.2. Experiment ……...… 54

4.2.1. Hydrogels …..…… 54

4.2.2. HA solution ……..... 55

4.2.3. *In situ* observation system for frictional interface …….....… 55

4.3. Results and Discussion …….. 55

4.3.1. *In situ* observation during oscillatory motion -effect of strain amplitude- ……..……..…….55

4.3.2. *In situ* observation during oscillatory motion -effect of angular frequency- ……....56

4.4. Conclusion ……. 56

References …… 57

Figures …….. 58

Chapter 5. General Conclusion ……... 62

List of Publications ……...…… 64

Acknowledgement …… 65

Chapter 1. General Introduction

Friction is a universal phenomenon in which a force acts in a direction to prevent relative motion when an object is in contact. Solid friction, as represented by the Ammonton-Coulomb's law, is the mainstream of friction research, however, reports on the friction of soft matter have been increasing[1-5]. Soft matter is a material like colloid, gels, polymers, granular materials, and so on. For example, hydrogels are polymer networks containing large amounts of water. The networks are formed by chemical and/or physical cross-linking between polymer chain. Due to soft and wet properties of hydrogels, they are highly close to biological tissues. Furthermore, the discovery of volume phase transition by Tanaka *et al.*[6], hydrogels are widely expected to be applied in the medical field.

. In our laboratory, not only the development of high-strength hydrogels, but also the surface friction of hydrogel has been studied[7-10]. A frictional coefficient of hydrogels is smaller than those observed in solid materials. The surface friction of gels is comparable to that in human body. Friction in the human body so smoothly that we do not notice, such as blood flow, joint motion, eyes blinking, and so on. The excellent friction reductions in biological systems are achieved by the soft and hydrated biological tissues and hydrated biopolymers as lubricants. For example, in knee joints, lubrication by synovial fluid that occupies the space between the articular cartilages decreases friction between them[11]. Therefore, if we could understand the mechanism of low friction of human body through the researches of gel friction, it will be expected to contribute to the realization of an energy-saving society.

Here, there are two problems. One is that average value of unidirectional motion has been mainly analyzed in past friction studies. The other is that there are few suitable analysis methods due to the complexity of the non-linear response of soft matter. However, recent 20 years, the developments of an equipment and the advances of analysis methods is changing the situation. In particularly, Fourier-transform rheology[12] and large amplitude oscillatory shear (LAOS)[13,14] is very important method. Both methods have a similar concept of directly analyzing the raw data of non-linear response.

In this study, the analysis of an energy dissipation during oscillatory friction was reached. The chapters are described below. This dissertation comprises five chapters including this general introduction as **Chapter 1**.

In **Chapter 2**, a transition from linear response to non-linear response of gel friction in water was confirmed from strain sweep test. For a more detailed analysis, I obtained stress-strain Lissajous curves at some strain amplitude. From the analysis of two dimensionless parameter, it was found that gel friction in water had two energy dissipation mode, one was microscopic slip at small strain region, another was macroscopic slide.

In **Chapter 3**, The friction of the gel in the concentrated hyaluronic acid (HA) solution was studied in consideration of the experiment in the environment closer to the biological joint. From the analyses, it was found that the HA layer remained at gel/glass interface was important for the gel friction in HA solution.

In **Chapter 4**, contact pattern formation at frictional interface between gel and glass in concentrated HA solution was observed on oscillatory shearing. Contact patterns have been observed only in uni-directional rotation. On Oscillatory shearing, I found that the contact pattern formation had a threshold of strain amplitude.

Finally, the conclusion and the contribution of this dissertation is summarized in **Chapter 5**, General conclusion.

References

1 A. Singh, M. Corvelli, S. A. Unterman, K. A. Wepasnick, P. McDonnell and J. H. Elisseeff, "Enhanced lubrication on tissue and biomaterial surfaces through peptide-mediated binding of hyaluronic acid." *Nat. Mater.*, **2014**, *13*, 988-995

2 J. Kim and A. C. Dunn, "Soft hydrated sliding interfaces as complex fluids." *Soft Matter.*, **2016**, *12*, 6536-6546.

3 H. M. Shewan, J. R. Stokes and M. Cloitre, "Particle-wall tribology of slippery hydrogel particle suspensions." *Soft Matter.*, **2017**, *13*, 2099-2106.

4 J. M. Uruena, E. O. McGhee, T. E. Angelini, D. Dowson, W. G. Sawyer and A. A. Pitenis "Normal Load Scaling of Friction in Gemini Hydrogels." *Biotribology*, **2018**, *13*, 30-35.

5 Y. A. Meier, K. Zhang, N. D. Spencer and R. Simic, "Linking Friction and Surface Properties of Hydrogels Molded Against Materials of Different Surface Energies." *Langmuir*, **2019**, *35*, 15805-15812.

6 T. Tanaka, "Phase transition in gels and a single polymer." *Polymer*, **1979**, *20* (11), 1404-1412.

7 J. P. Gong, M. Higa, Y. Iwasaki, Y. Katsuyama and Y. Osada, "Friction of Gels." *J. Phys. Chem. B*, **1997***, 101* (28), 5487-5489.

8 J. P. Gong and Y. Osada, "Gel friction: A model based on surface repulsion and adsorption." *J. Chem. Phys.*, **1998**, *109* (18), 8062-8068.

9 J. P. Gong and Y. Osada, "Surface friction of polymer gels." *Prog. Polym. Sci.*, **2002**, *27*, 3-38.

10 J. P. Gong, "Friction and lubrication of hydrogels – its richness and complexity." *Soft Matter*, **2006**, *2*, 544-552.

11 A. G. Ogston and J. E. Stanier, “The physiological function of hyaluronic acid in synovial fluid; viscous, elastic and lubricant properties.” *J. Physiol.*, **1953**, *119*, 244-252.

12 M. Wilhelm, P. Reinheimer and M. Ortseifer, “High sensitivity Fourier-transform rheology.” *Rheol. Acta*, **1999**, *38*, 349-356.

13 R. H. Ewoldt, A. E. Hosoi and G. H. McKinley, “New measure for characterizing nonlinear viscoelasticity in large amplitude oscillatory shear.” *J. Rheol.*, **2008**, *52* (6), 1427-1458.

14 K. Hyun, M. Wilhelm, C. O. Klein, K. S. Cho, J. G. Nam, K. H. Ahn, S. J. Lee, R. H. Ewoldt and G. H. McKinley, “A review of nonlinear oscillatory shear tests: Analysis and application of large amplitude oscillatory shear (LAOS).” *Prog. Polym. Sci.*, **2011,** *36*, 1697-1753.

Chapter 2. Non-Linear Analysis of Frictional Interface of Gel in Water

2.1 Introduction

It is generally well known that the soft matter shows linear response with small strain and non-linear response with large strain. Therefore, the strain sweep test is a conventional method to obtain the threshold strain of linear to non-linear responses of soft matter[1,2]. However, in friction research field, strain sweep test for frictional interface has been not found. So, I investigated strain sweep frictional test to gel/glass interface.

Additionally, average analysis of unidirectional motion has been the mainstream in past friction studies. Using average analysis, it is unclear how the material behaves in the nonlinear response. Here, I adopt analyses stress-strain Lissajous curves at some strain amplitude. Analyzing Lissajous curves obtained from an oscillatory motion is an important method to understand non-linear rheology of soft matter[3]. Stress-strain Lissajous curve is also useful for analyzing a friction, which is a process of energy dissipation. Furthermore, Non-linearity and energy dissipation are characterized by the two dimensionless parameters.

2.2 Experiments

2.2.1 Materials

Polyvinyl alcohol (PVA) (M_w = 88,000, degree of polymerization = 2,000, degree of saponification > 99 %) was purchased from Nacalai Tesque, Inc. Schematic illustrations of PVA was shown in Fig. 2-1. Dimethyl silicone oil (KF-96H-100000CS) was purchased from Shin-Etsu Chemical Co., Ltd. It was used as a standard viscous sample. Dimethyl sulfoxide (DMSO) was purchased from Wako Pure Chemical Industries, Ltd. 1H, 1H, 2H,

2H – Perfluorodecyltrichlorosilane (FDTS) was purchased from Alfa Aeser Inc. Deionized water (Milli-Q) was used. All the materials were used without purification.

2.2.2 Preparation of hydrogels

Physically crosslinked PVA gels were used in this study, which were prepared by a quenching method from PVA solution of a solvent mixture (DMSO: H_2O = 3: 1, w/w)[4]. The initial PVA concentration was 10 wt%. First, PVA flakes were added in the solvent mixture stirred at room temperature. After stirring for 30 minutes, that mixture was heated at 90 ℃ for 1 hour to dissolve the PVA flakes. Water and DMSO vapors were recovered with a condenser during heating. Then, PVA solution was degassed in a vacuum oven and poured into a mold consisting of two glass plates (10 cm × 10 cm) with a silicone rubber spacer (3.0 mm). After that, this mold was quenched at a freezer of -40 ℃ for 16 hours to form physically crosslinked gel. The mold was then warmed to room temperature and the gel sheet was removed and immersed in a large amount of water. Water was exchanged dairy to extract DMSO in the gel sheet for one week. The equilibrium thickness of the gel in water was 2.4 mm.

2.2.3 Frictional substrate

A hydrophobically treated cover glass (Micro-cover glass C050701, Matsunami Glass Co., Ltd.) was used as the rigid counter substrate in the friction test. For the surface treatment, these glass pieces were firstly cleaned in an ozone cleaning chamber (UV/O3). To prepare the hydrophobic surface, the cleaned glasses were exposed to a binding silane vapor, FDTS, at 20 kPa for 8 h in a vacuum desiccator. The contact angle to water of the treated glass was 110 ± 2°.

2.2.4 Compression test

To measure Young's modulus E of PVA gels, a compression test was performed with a universal mechanical test machine (Tensilon RTC-1310A, Orientec Co.). Cylindrical gel with a 15-mm diameter and 2.4-mm thickness was compressed with a constant velocity of 0.2 mm/min to strain ~ 50%. The modulus data was the average over 3 samples. E of PVA gels was 54 kPa.

2.2.5. Viscosity measurement

The viscosity of silicone oil was measured by a rheometer ARES-G2 (TA instruments) with cone-plate geometry (diameter: 50 mm) with steady rotation mode at 25 ℃. The shear rate $\dot{\gamma}$ varied from 10^{-3} to 10^{3} s^{-1}. The viscosity of silicone oil was 98 Pa s.

2.2.6 Dynamic viscoelasticity measurement

The dynamic viscoelasticity of PVA gel was measured by ARES-G2 with parallel-plate (diameter: 25mm) at 25 ℃. Measurement method was the frequency sweep test in the angular frequency range ω of 0.1 ~100 rad s^{-1} at a shear strain of 0.1%.

2.2.7. Strain sweep test

The schematic illustration of the oscillatory frictional test using ARES-G2 is shown in Fig. 2-2. A hydrophobically-treated cover glass was a frictional substrate against PVA gel. Cylindrical PVA gels, which were 15 mm in diameter and 2.4 mm in thickness, whose center was aligned with the rotational axis of the rheometer, were fixed with a cyanoacrylate instant adhesive agent (Toagosei Co., Ltd.) to the lower plate of the

rheometer, and then water was poured on the top surface of the gel. Subsequently, the hydrophobically-treated glass was allowed to approach from above the gel at a velocity of 2 μm/s, and then was stopped when the normal pressure reached a preset value. A waiting time of 15 minutes was applied prior to the friction measurement, during which the normal pressure decreased slightly due to stress relaxation of the gel. To compensate for this change, the compression was adjusted slightly to maintain the preset normal pressure. The torque generated at the sliding gel/glass interface shown in Fig. 2-2 was measured by oscillating the lower plate.

In this test, the gels were applied with a sinusoidal shear strain of $\gamma(t) = \gamma_{max}\sin(\omega t)$ at an angular frequency $\omega = 1$ rad s^{-1} and a strain amplitude $\gamma_{max} = 10^{-4}$ to 10^{1}, and the torque T(t) was measured. The γ_{max} is defined as $\gamma_{max} = R\theta/h$, where h (= 2.4 mm) and R (= 7.5 mm) are the gel thickness and the radius of the apparent contact area of the gel, respectively, θ is the maximum rotational angle and γ_{max} was varied by changing θ. The frictional force F was calculated from the torque as $F = 4T/3R$ [5]. The frictional stress σ was calculated as $\sigma = 4T/3\pi R^3$. The oscillatory shear stress amplitude σ_{max} was obtained assuming a linear viscoelastic response of the measured systems, $\sigma = \sigma_{max}\sin(\omega t+\delta)$. Measurements were performed in pure water with normal pressures of 11, 22, 33, and 44 kPa. Measurement temperature was controlled at 25 ℃.

Furthermore, as a control experiment, strain sweep test was also performed on the PVA gel with its top surface and bottom surface fixed to the upper and lower plates of the rheometer. Such test on fixed gel without any slip reveals the bulk dynamic mechanical properties of the PVA gel. Hereafter, we refer to the gels with the bottom surface fixed and upper surface unfixed for friction test as slidable gels and the gel with two surfaces fixed as fixed gel.

2.2.8 Oscillatory test for Lissajous curves

Oscillatory tests to obtain stress-strain Lissajous curves were performed. At this test, the samples were applied with an oscillatory sinusoidal shear of $\gamma = \gamma_{max}\sin(\omega t)$ at an angular frequency $\omega = 1$ rad s^{-1}, at a specific strain γ_{max} for 20 cycles, and the stresses obtained in the 20th cycle were plotted against the applied shear strain. Measurements for friction of gel in water were performed at a normal pressure of 33 kPa.

2.2.9 *In situ* observation system for frictional interface

An *in situ* observation system for frictional interface[6] will be introduced. Fig. 2-3 shows schematic illustration of the observation of gel-glass contact based on the principle of critical refraction using a trapezoidal prism. This system utilizes the principle of the critical refraction between different materials. In Fig. 2-3(a), where a water film exists at the gel-glass interface, the light coming from the water side refracts at the angle less than the critical refractive index of water to glass θ_{water} defined by following formula.

$$\theta_{water} = n_{water} / n_{glass} \qquad (2\text{-}1)$$

On the other hand, in Fig. 2-3(b) where the gel contacts with the glass prism, the light comes from the gel refracts at the angle less than the critical refractive index of gel to glass θ_{gel} defined by a following formula.

$$\theta_{gel} = n_{gel} / n_{glass} \qquad (2\text{-}2)$$

Here, n_{water} and n_{gel} are the refractive indexes of water and gel, and those values are 1.332 and 1.358, respectively. $\theta_{water} < \theta_{gel}$. So, when we set a camera at an angle θ_r ($\theta_{water} < \theta_r < \theta_{gel}$), a black image is observed in Fig. 2-3(a), and a bright image of the gel is observed in Fig. 2-3(b). Therefore, the difference in the critical angle of refraction

between water and glass and between gel and glass can distinguish where the gel is in contact with glass from where it is not.

A schematic illustration of the *in situ* observation system using a rheometer is shown in Fig. 2-4. To obtain images of frictional interface, an observation was performed by using a digital video camera (Sony Co. Ltd,). The camera was set up the angle θ_r satisfied the condition $\theta^c_{water} < \theta_r < \theta^c_{gel}$. A trapezoidal prism was attached to the upper plate of the rheometer. A hydrophobically-treated cover glass was fixed to the bottom of the trapezoidal prism. The rest of measurement preparation procedure is same as described at 2.2.7.

2.3 Results and Discussion

2.3.1. Dynamic viscoelasticity of PVA gel

Fig. 2-5 shows dynamic viscoelasticity of PVA gel. *G*' is more than 10 times larger than *G*" in whole angular frequency region. Therefore, PVA gel in this study is an elastic material at 25 ℃.

2.3.2 Strain sweep test

Figure 2-6 shows the log-log plot of stress amplitude σ_{max} vs strain amplitude γ_{max} curves measured by the strain sweep test for slidable gel in pure water and fixed gel. In the case of the fixed gel, the stress-strain curve corresponds to the bulk deformation. A straight line with a slope of 1.0 was observed up to a large strain (~0.5), and then a slight strain-hardening was observed at larger strains. For the friction of gel in water, the slope of stress-strain curves was also 1.0 in the small strain region as for the fixed gel. However,

the stress-strain curves deviated from linearity and showed a strong strain softening at large strains. Specifically, the critical strain amplitude for the deviation from linearity occurred at quite a large value ($\gamma_{max,c}$ = 1) and above this strain the stress started to decrease. Furthermore, the stresses of the slidable gel in water were slightly lower than the fixed gel, almost independent of the normal pressure in the range of 11~44 kPa. The deviation from the linearity suggests the slide of the gel under shear motion. Here, I introduced an analysis of stress-strain Lissajous curve.

2.3.3. Lissajous curves

To analyze the non-linear viscoelastic response and determine if the critical strain, $\gamma_{max,c}$ observed in Figure 2-6 corresponds to the transition from a linear to a non-linear response, I performed the oscillatory test and obtained the stress-strain Lissajous curves. A linear response gives a stress-strain Lissajous curve in an elliptical shape, while a non-linear response results in a distortion from the elliptical shape. Therefore, from the shape of the Lissajous curve, we can determine the critical strain for the transition from the linear response to the non-linear response with the increase of the strain amplitude for each system. Furthermore, the behavior of energy dissipation can also be characterized from Lissajous curves.

As a typical example, Figure 2-7 shows the sinusoidal curves for stress, strain, and strain rate of the oscillatory test as a function of time (Fig. 2-7[a]), and the corresponding Lissajous curves (Figs. 2-7[b] and 2-7[c]) of the slidable gel in water around the transition strain $\gamma_{max,c}$ = 1. The strain rate curve was calculated from the strain

curve by taking the derivative with respect to time, and the strain rate reached a maximum at strain 0. The stress curve showed a phase shift relative to the strain curve, and furthermore, the shape of the stress curve was distorted from the sinusoidal, indicating the non-linear viscoelastic response of the slidable gel around the transition strain. The stress-strain Lissajous curve rotated with time in a clockwise direction (Fig. 2-7[b]), while the stress-strain rate Lissajous curve rotated with time in a counter-clockwise direction (Fig. 2-7[c]). Slight distortion from the elliptical shape was also observed in these Lissajous curves.

Figure 2-8 to Figure 2-10 shows the stress-strain Lissajous curves at varied maximum strain γ_{max} for different systems. Figure 2-8 showed the Lissajous curves of the silicone oil. The Lissajous curves showed good elliptical shapes. Furthermore, if stress $\sigma(t)$ and strain $\gamma(t)$ of these Lissajous curves are normalized with stress amplitude σ_{max} and strain amplitude γ_{max}, these Lissajous curves will be circles, indicating that the silicone oil was viscous fluid. On the other hand, from Figure 2-9, the Lissajous curves of the fixed gel, which indicated the deformation of the gel, were almost linear lines, showing no hysteresis loop. This result confirms that the gel is hyper-elastic with negligible energy dissipation during deformation. Figsure 2-10 showed the Lissajous curves of slidable gel in water. The Lissajous curves of slidable gel in water are approximately elliptical when $\gamma_{max} < \gamma_{max,c} = 1$ (Fig. 2-10[a]) and become distorted to parallel square shape when $\gamma_{max} > \gamma_{max,c}$ (Fig. 2-10[b]). This clearly confirms the interfacial slip of the slidable gel at $\gamma_{max} > \gamma_{max,c}$. It was surprising that large hysteresis loops were observed, even in the regime of $\gamma_{max} < \gamma_{max,c}$ where the Lissajous curves are in elliptical shapes, which is quite different from the behaviors of fixed gel that did not show hysteresis. This indicates that even in the small strain regime where the stress-strain

curves obey linearity, the slidable gels already dissipate energy at the interface. In addition, it should be noticed that the maximum stress σ_{max} on Lissajous curves reached the highest value at $\gamma_{max,c} = 1$ and decreased at larger γ_{max}. This behavior is consistent with the results shown in Fig. 2-6.

2.3.4. Two dimensionless parameters for analysis of Lissajous curves

To characterize the Lissajous curves from the viewpoint of non-linearity and energy dissipation, I used two dimensionless quantities; one was the strain hardening ratio, *S*, that characterizes the non-linearity of the Lissajous curves[7].

$$S = \frac{G'_L - G'_M}{G'_L} \qquad (2\text{-}3)$$

As shown in Figure 2-11, G'_L and G'_M are secant gradients at maximum strain and tangent gradients at zero strain on the Lissajous curves, respectively; G'_L and G'_M correspond to the elastic moduli in large and small deformation, respectively. An *S* value of 0 indicates a linear elastic response, a value > 0 indicates intracycle strain stiffening, and a value < 0 indicates intracycle strain softening.

Prior to the introduction of the other parameter, I will show the energy dissipation density E_d (J/m^3) estimated from one cycle Lissajous curve. First, E_d is defined the area of stress-strain Lissajous curve, and that is shown the equation below.

$$E_d = \int_{cycle} \sigma(t) d\gamma \qquad (2\text{-}4)$$

Here, σ is stress and γ is strain, respectively. Eq. 2-4 changes to

$$E_d = \int_{cycle} \sigma(t) \frac{d\gamma}{dt} dt$$

$$= \int_0^{\frac{2\pi}{\omega}} \sigma(t)\dot{\gamma}(t)dt \qquad (2\text{-}5)$$

Assuming that applying sinusoidal strain $\gamma(t) = \gamma_{max}\sin(\omega t)$ and sinusoidal stress $\sigma(t) = \sigma_{max}\sin(\omega t+\delta)$ corresponding to a linear viscoelastic response,

$$E_d = \int_0^{\frac{2\pi}{\omega}} \sigma_{max} \sin(\omega t + \delta)\, \omega\gamma_{max} \cos(\omega t)\, dt \qquad (2\text{-}6)$$

Using $\sin\alpha\cos\beta = \frac{\sin(\alpha+\beta)+\sin(\alpha-\beta)}{2}$,

$$E_d = \frac{\omega\sigma_{max}\gamma_{max}}{2} \int_0^{\frac{2\pi}{\omega}} \{\sin(2\omega t + \delta) + \sin\delta\}\, dt$$

$$= \frac{\omega\sigma_{max}\gamma_{max}}{2} \left[\left\{-\frac{1}{2\omega}\cos(2\omega t + \delta)\right\} + t\sin\delta\right]_0^{\frac{2\pi}{\omega}}$$

$$= \frac{\omega\sigma_{max}\gamma_{max}}{2} \left\{-\frac{\cos(4\pi+\delta)-\cos\delta}{2\omega} + \frac{2\pi}{\omega}\sin\delta\right\}$$

$$= \sigma_{max}\gamma_{max}\pi\sin\delta. \qquad (2\text{-}7)$$

From the definition of G" $\left(G' = \frac{\sigma_{max}}{\gamma_{max}}\cos\delta,\ G" = \frac{\sigma_{max}}{\gamma_{max}}\sin\delta, \frac{G"}{G'} = \tan\delta\right)$,

$$E_d = \pi\gamma_{max}^2 \cdot \frac{\sigma_{max}}{\gamma_{max}}\sin\delta$$

$$= \pi G"\gamma_{max}^2 \qquad (2\text{-}8)$$

From Eq. 2-8, The slope of plotting E_d against γ_{max} for linear viscoelastic material should show 2.

The other dimensionless quantity is an energy dissipation occupancy, κ, that characterize the relative energy dissipation in one cycle of the oscillatory test.

$$\kappa = \frac{E_d}{2\sigma_{max} \cdot 2\gamma_{max}} \qquad (2\text{-}9)$$

Here, the denominator $2\sigma_{max} \cdot 2\gamma_{max}$ in Eq. 2-9 is the area of the rectangle circumscribing the Lissajous curve, as shown in Fig. 2-12. For an elastic system, E_d is zero, while the E_d of a linear viscoelastic material scales to γ_{max} with an exponent of 2 [8,9]. As E_d depends on the moduli of the system, it prevents the comparison of the energy dissipation mechanism between different systems, while κ, the newly introduced parameter, enables the comparison of different systems. The κ takes values in the range of 0-1. For ideal elastic materials that show straight lines of Lissajous curves, κ is 0 because there is no energy dissipation. Whereas, for ideal viscous materials that have an elliptical shape of Lissajous curves, κ is $\pi/4 \approx 0.785$. For the linear viscoelastic material, κ has a value in the range of $0 < \kappa < 0.785$, whereas for a non-linear viscoelastic system, κ could be > 0.785.

The strain γ_{max} dependences of S, E_d and κ are shown in Figs. 2-13, 2-14 and 2-15, respectively. For the fixed PVA gel, S was almost zero at the small strain regime but began to increase at a large strain regime, while the κ maintained a value of zero for the entire strain range. This confirms that the PVA gel is a hyper-elastic material, showing a linear response at a small strain, a non-linear response at a large strain, and negligible energy dissipation in the entire strain range. For the slidable gel in water, S was almost zero at the small strain regime, however it increased abruptly when the strain γ_{max} exceeded the critical strains $\gamma_{max,c} = 1.0$, indicating the transition from linear to non-linear

responses. Surprisingly, κ values were around 0.5 even in the small strain ($\gamma_{max} < \gamma_{max,c}$), i.e., they were much higher than zero. This differed from the behaviors of the fixed gel. From the $S = 0$ and $\kappa > 0$, the response of the slidable gel in water was characteristic to a linear viscoelastic system at small strain. Furthermore, κ increased rapidly at large strain ($\gamma_{max} > \gamma_{max,c}$) and was across the red line for ideal viscous materials ($\kappa = 0.785$) and saturated to $\kappa = 0.9$. From the large S and κ, the slidable gel in water was strongly non-linear viscoelastic at a large strain, indicating the macroscopic sliding of the interface. These are shown in Fig. 2-16 to 2-18. The bright area of these figures shows a contact interface between the hydrogel and the glass substrate under applied shear strain in water. The increase of κ indicates that the sliding area was growing from the periphery of the hydrogel cylinder with increasing applied shear strain. The shear strain at which the hydrogel surface began to slide varied according to the distance from the rotation axis. It was clarified that the increase of the sliding area corresponded to the increase of the κ value.

The results show that the slidable gel in water displayed linear viscoelastic behavior at $\gamma_{max} < \gamma_{max,c} = 1$ and a non-linear viscoelastic behavior at $\gamma_{max} > \gamma_{max,c}$. The latter corresponds to the slide of the interface. Therefore, what is the energy dissipation mechanism even prior to the occurrence of slide? For the slidable PVA gel in water, there was direct adsorption of the polymer strands on the surface of PVA gel to the hydrophobically treated glass substrate[10]. The dynamic adsorption-desorption provides a self-healing interface. With the absence of shearing deformation, the adsorption-desorption dynamics are in equilibrium and there is no energy dissipation. Under the oscillatory shear deformation, the linear viscoelastic response was observed when the oscillatory frequency was comparable to the adsorption-desorption dynamics. In the large

strain region in which the slide occurs, the frictional resistance of the gel comes from the elastic deformation of adsorbed polymer strands[11]. When the adsorbed polymer strands are detached from the substrate under shearing, the stored elastic energy of the strands is released and the energy is converted to heat, contributing to energy dissipation. The existence of a critical strain for the transition from linear response to the non-linear response indicates static-like friction behavior.

2.4 Conclusion

From the result of strain sweep tests, frictional interface of gel in water was almost not depend applied normal pressure because of rapid squeezing of water from interface. Furthermore, I have clarified a critical strain amplitude $\gamma_{max,c}$ which transited from linear response to non-linear response.

The Lissajous curves at each system showed various shapes. To quantify the shapes of Lissajous curves, two dimensionless parameters S and κ were utilized. From these analyses, gel friction in water can be distinguished between microscopic slip due to dynamic adsorption-desorption between polymer strands and glass surface, and macroscopic slide of gel/glass interface.

References

1 S. P. Meeker, R. T. Bonnecaze and M. Cloitre, "Slip and Flow in Soft Particle Pastes." *Phys. Rev. Lett.*, **2004**, *92* (19), 198302.

2 C. Storm, J. J. Pastore, F. C. MacKintosh, T. C. Lubensky and P. A. Janmey, "Nonlinear elasticity in biological gels." *Nature*, **2005**, *435*, 191-194.

3 K. Hyun, M. Wilhelm, C. O. Klein, K. S. Cho, J. G. Nam, K. H. Ahn, S. J. Lee, R. H. Ewoldt and G. H. McKinley, "A review of nonlinear oscillatory shear tests: Analysis and application of large amplitude oscillatory shear (LAOS)." *Prog. Polym. Sci.*, **2011,** *36*, 1697-1753.

4 H. Trieu and S. Qutubuddin, "Poly(vinyl alcohol) hydrogels: 2. Effects of processing parameters on structure and properties." *Polymer*, **1995**, *36* (13), 2531-2539.

5 J. P. Gong, G. Kagata and Y. Osada, "Friction of Gels. 4. Friction on Charged gels." *J. Phys. Chem. B*, **1999**, *103* (29), 6007-6014.

6 T. Yamamoto, T. Kurokawa, J. Ahmed, G. Kagata, S. Yashima, Y. Furukawa, Y. Ota, H. Furukawa and J. P. Gong, "*In situ* observation of a hydrogel-glass interface during sliding friction." *Soft Matter*, **2014**, *10*, 5589-5596.

7 R. H. Ewolt, A. E. Hosoi and G. H. McKinley, "New measures for characterizing nonlinear viscoelasticity in large amplitude oscillatory shear." *J. Rheol.*, **2008**, *52* (6), 1427-1458.

8 S. N. Ganeriwala and C. A. Rotz, "Fourier transform mechanical analysis for determining the nonlinear viscoelastic properties of polymers." *Polym. Eng. Sci.*, **1987**, *27* (2), 165-178.

9 F. Yziquel, P. J. Carreau and P. A. Tanguy, "Non-linear viscoelastic behavior of

fumed silica suspensions." *Rheol. Acta*, **1999,** *38*, 14-25.

10 T. Tominaga, N. Takedomi, H. Biederman, H. Furukawa, Y. Osada and J. P. Gong, "Effect of substrate adhesion and hydrophobicity on hydrogel friction." *Soft Matter*, **2008,** *4*, 1033-1040.

11 J. P. Gong and Y. Osada, "Surface friction of polymer gels." *Prog. Polym. Sci.*, **2002,** *27*, 3-38.

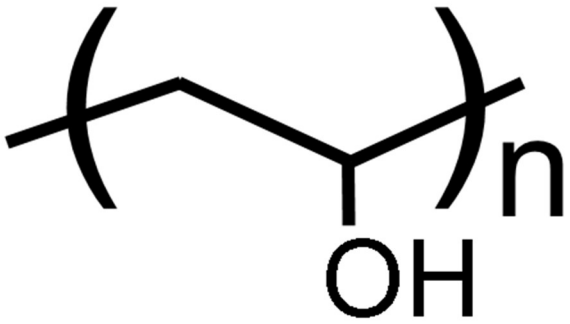

Figure 2-1. Chemical structure of PVA.

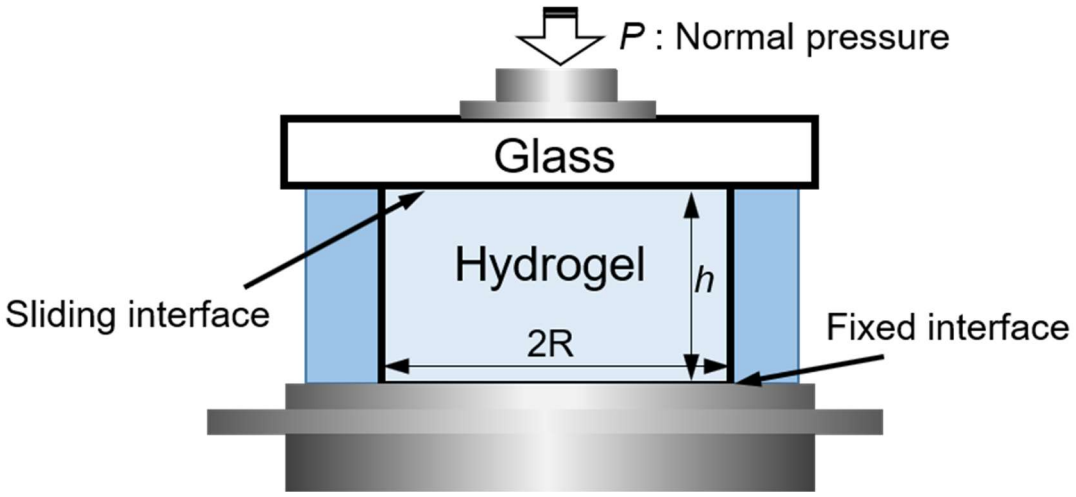

Figure 2-2. Schematic illustration of a set up for oscillatory frictional test.

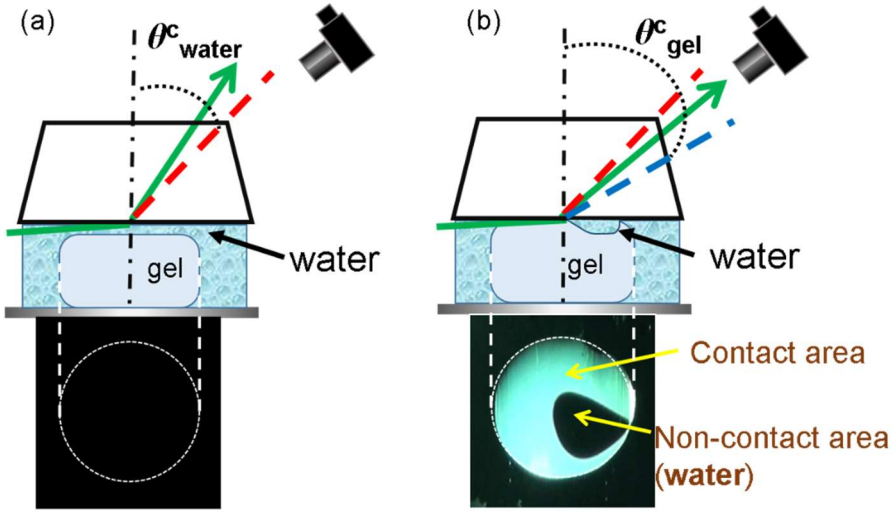

Figure 2-3. Schematic illustration of the observation of gel-glass contact based on the principle of critical refraction using a trapezoidal prism. In (a), where a water film exists at the gel-glass interface, the light coming from the water film refracts at the angle less than θ^c_{water}. On the other hand, in (b) where the gel contacts with the glass prism, the light comes from the gel refracts at the angle less than θ^c_{gel}. Here, θ^c_{water} and θ^c_{gel} are critical refraction angles of the water and water, respectively, and $\theta^c_{water} < \theta^c_{gel}$. So, when we set a camera at an angle θ_r ($\theta^c_{water} < \theta_r < \theta^c_{gel}$), a black image is observed in (a), and a bright image of the gel is observed in (b).

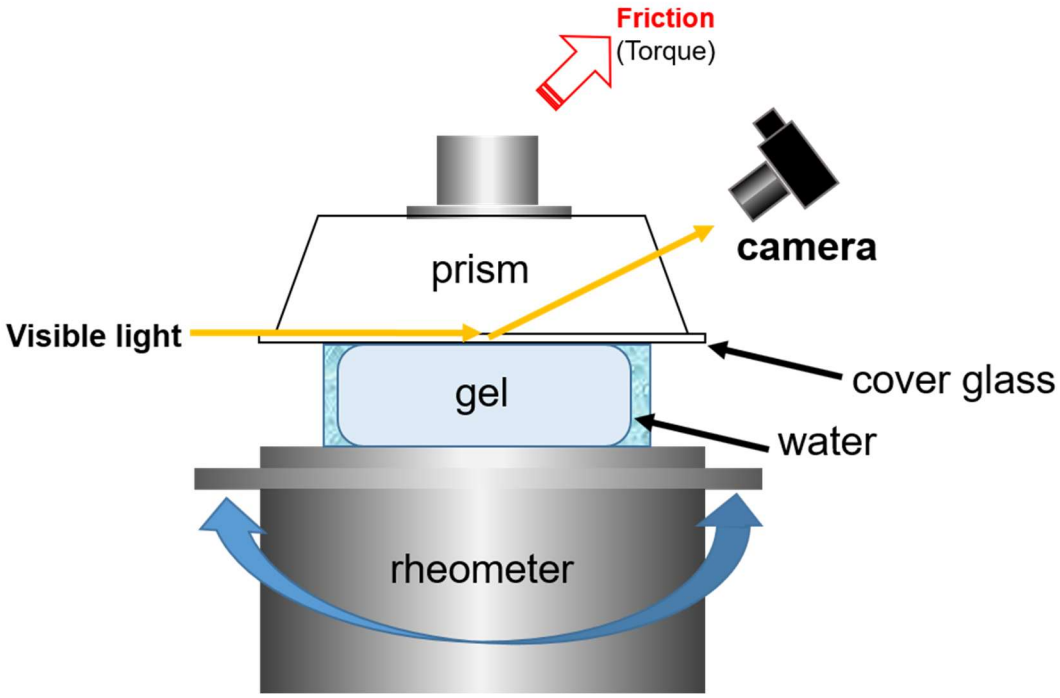

Figure 2-4. Schematic illustration of an *in-situ* observation system for frictional interface.

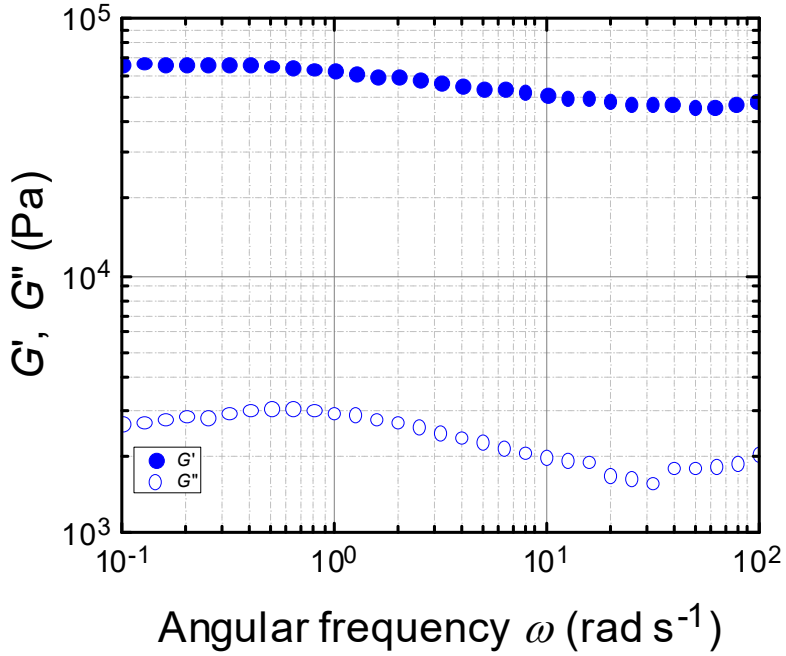

Figure 2-5. Dynamic viscoelasticity of PVA gel at 25 ℃. At this temperature, PVA gel is regarded an elastic material.

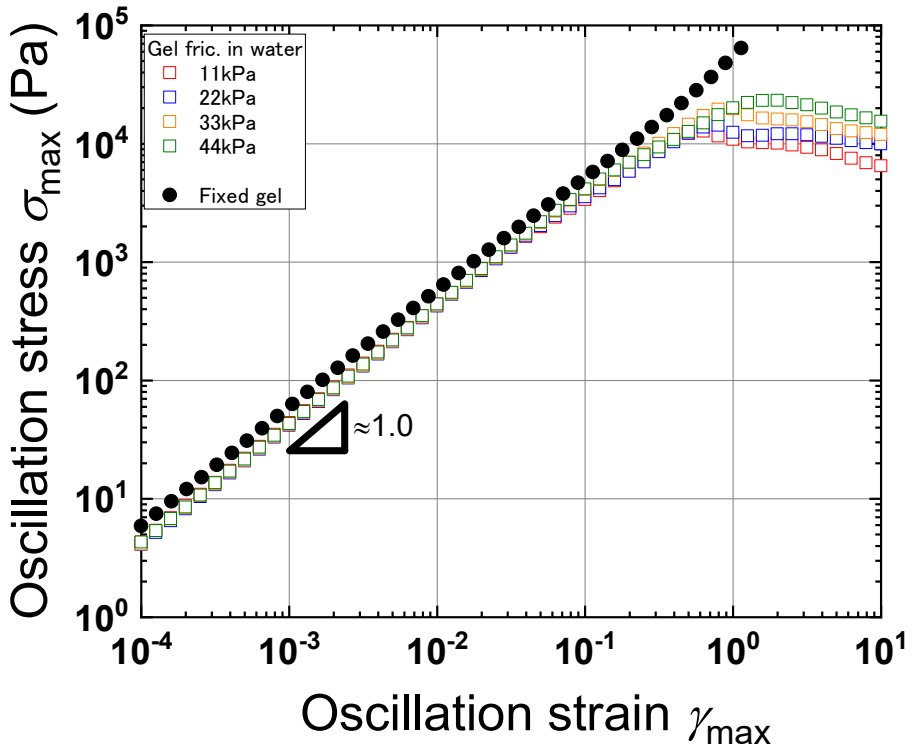

Figure 2-6. Strain sweep results of PVA hydrogel friction in water, measured by applying an oscillatory shear $\gamma_{max}\sin(\omega t)$. The σ_{max} is the maximum oscillatory shear stress assuming a linear viscoelastic response of the system. Black closed circles show the strain sweep test of PVA gel bulk deformation using fixed PVA gel. Note that $\omega = 1$ rad s^{-1} was adopted.

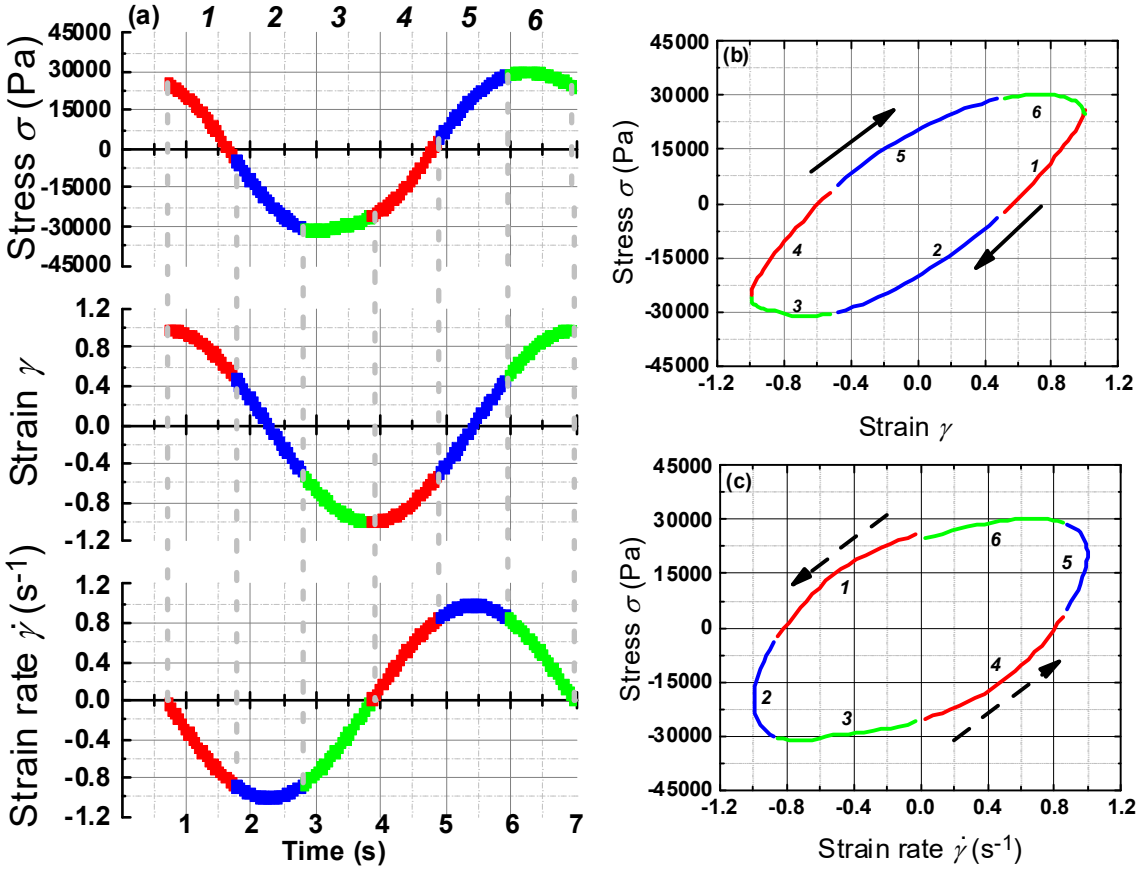

Figure 2-7. (a) Sinusoidal curves of applied strain (middle), strain rate (lower), and the shear stress generated (upper) obtained by oscillatory strain test with slidable poly (vinyl alcohol) (PVA) gel in water (angular frequency $\omega = 1$ rad s^{-1}, normal pressure 22 kPa). (b, c) The corresponding Lissajous curves of (b) strain-stress, and (c) strain rate-stress One cycle of sinusoidal curves for stress, strain, and strain rate was divided into six sections and shown with three colors. The stress-strain Lissajous curve rotates with time in a clockwise direction (black arrows), while the stress-strain rate Lissajous curve rotates with time in a counter-clockwise direction (dotted arrows).

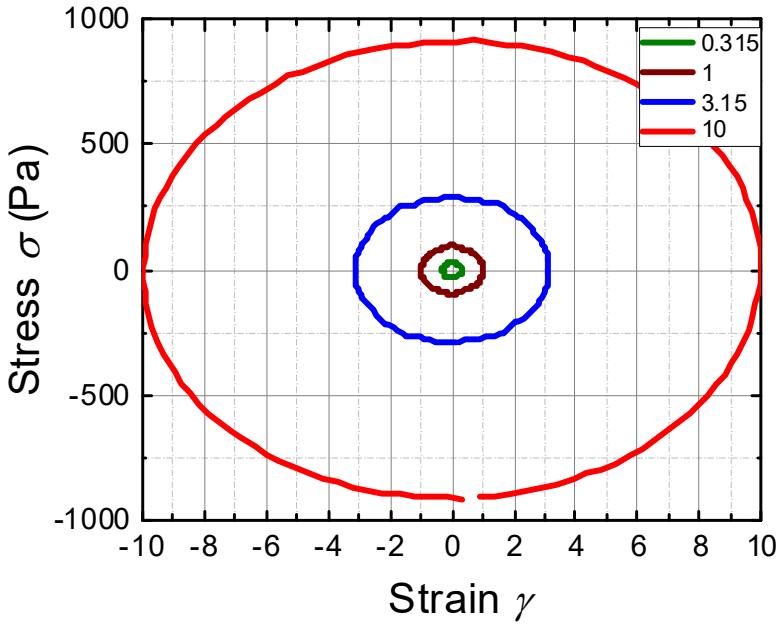

Figure 2-8. Stress-strain Lissajous curves of silicone oil. The numbers in the figures are the applied strain amplitude γ_{max}. Applied angular frequency was $\omega = 1$ rad s^{-1}.

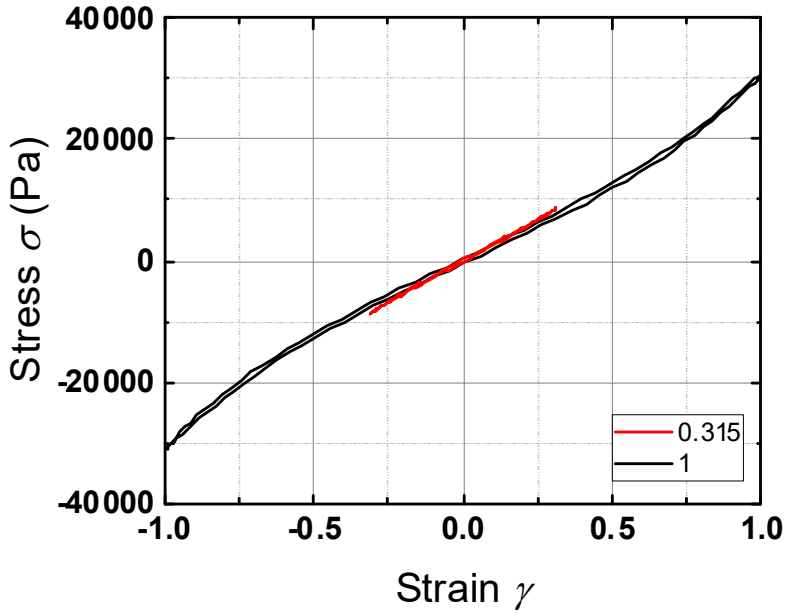

Figure 2-9. Lissajous curves of a fixed PVA gel. The numbers in the figures are the applied strain amplitude γ_{max}. Applied angular frequency was $\omega = 1$ rad s^{-1}.

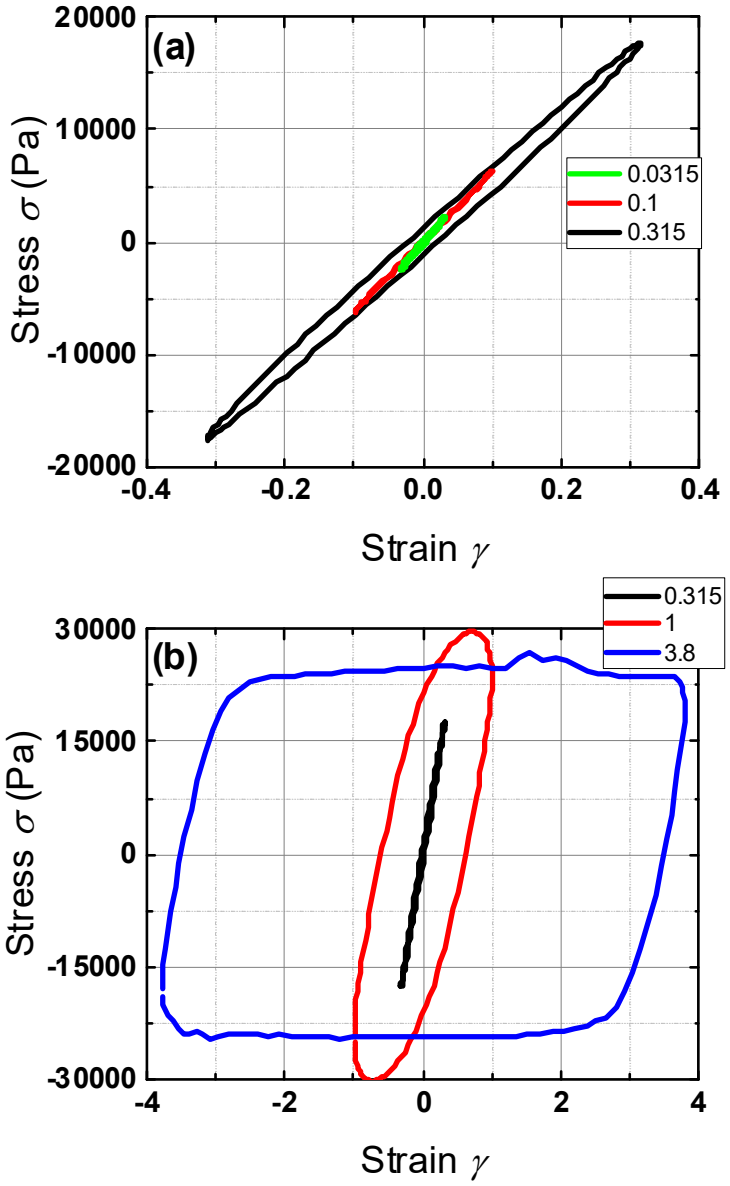

Figure 2-10. Lissajous curves of slidable gel in water at a normal pressure of 33 kPa. (a) small strain regime (b) large strain regime. The numbers in the figures are the applied strain amplitude γ_{max}. Applied angular frequency was $\omega = 1$ rad s^{-1}.

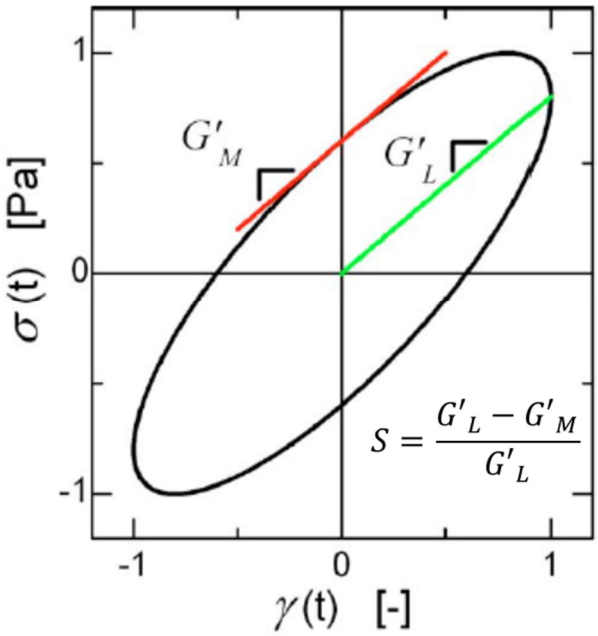

Figure 2-11. Characterization of non-linearity and energy dissipation of stress-strain Lissajous curves. Definition of the strain hardening ratio *S*, which characterizes the degree of non-linearity of elasticity.

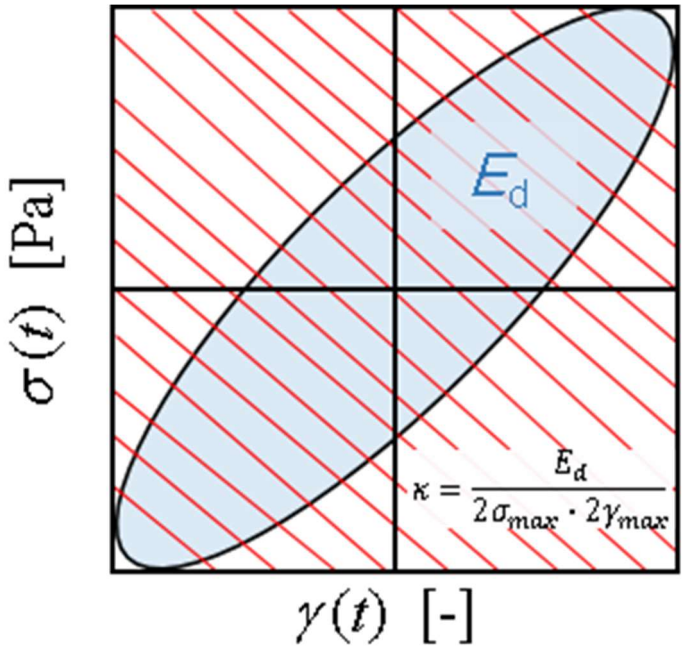

Figure 2-12. Definition of energy dissipation occupancy, κ, which characterizes the energy dissipation. The grey area enclosed by the stress-strain Lissajous curve stands for the energy dissipation density E_d for one cycle, and the red hatched area stands for $2\sigma_{max} \cdot 2\gamma_{max}$.

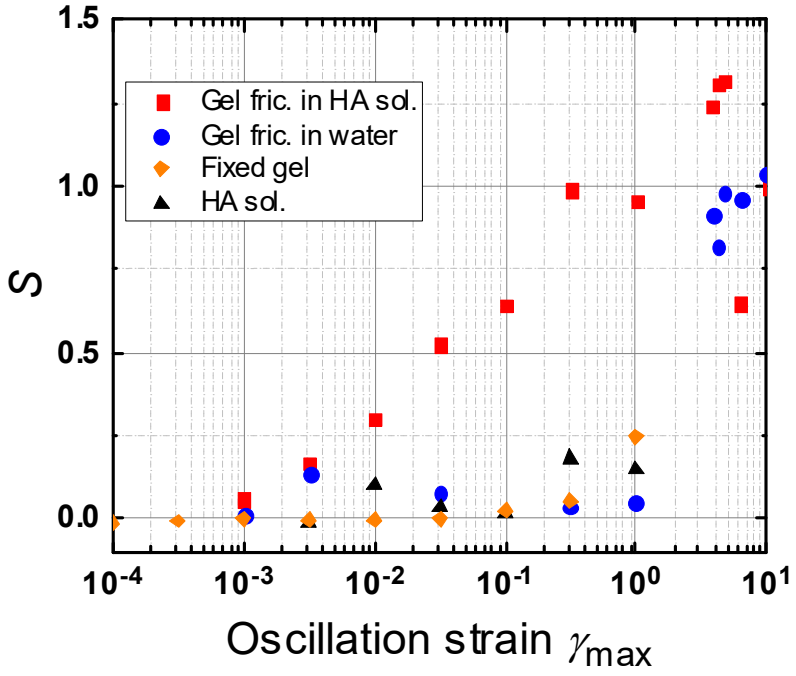

Figure 2-13. Oscillation strain dependence of S against applied maximum strain γ_{max} for various systems estimated from each Lissajous curves.

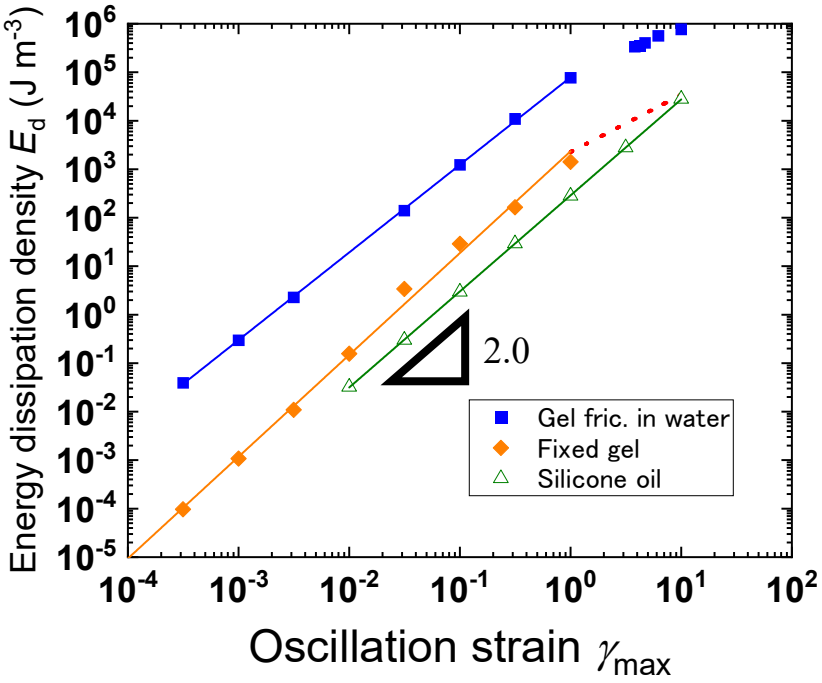

Figure 2-14. Oscillation strain dependence of an energy dissipation density E_d. E_d was estimated from 20th cycle Lissajous curves.

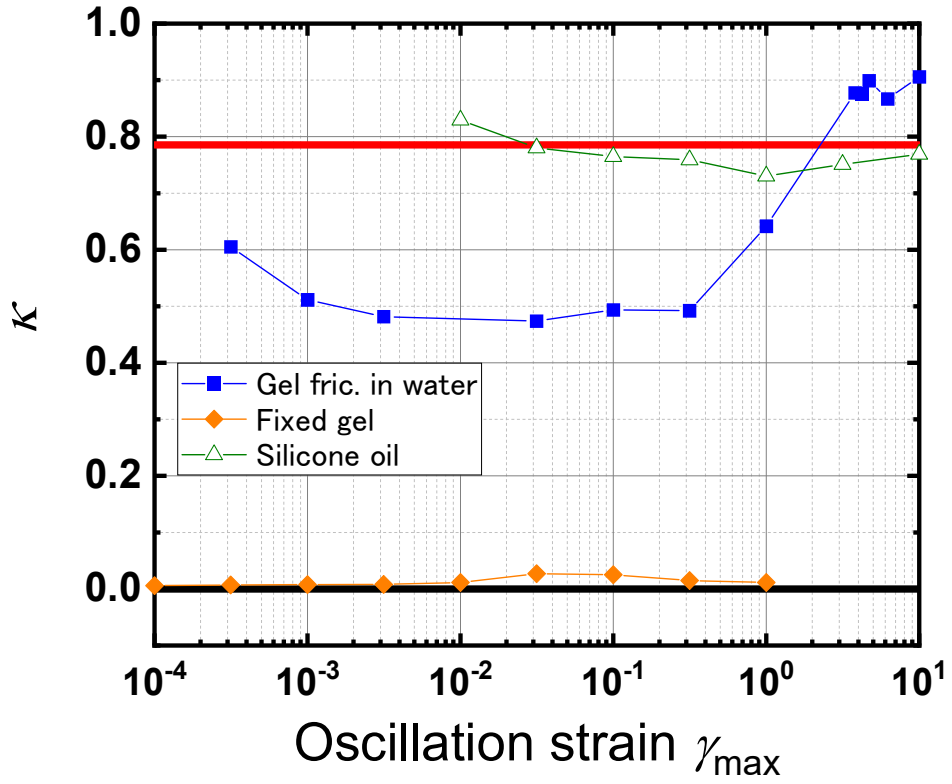

Figure 2-15. Oscillation strain dependence of occupancy parameter κ against applied strain amplitude γ_{max} for various systems estimated from each Lissajous curves. In this figure, the red line indicates κ = 0.785 for ideal viscous materials and the black line indicates κ = 0 for ideal elastic materials. The result of silicone oil is shown as a standard for the pure viscous liquid.

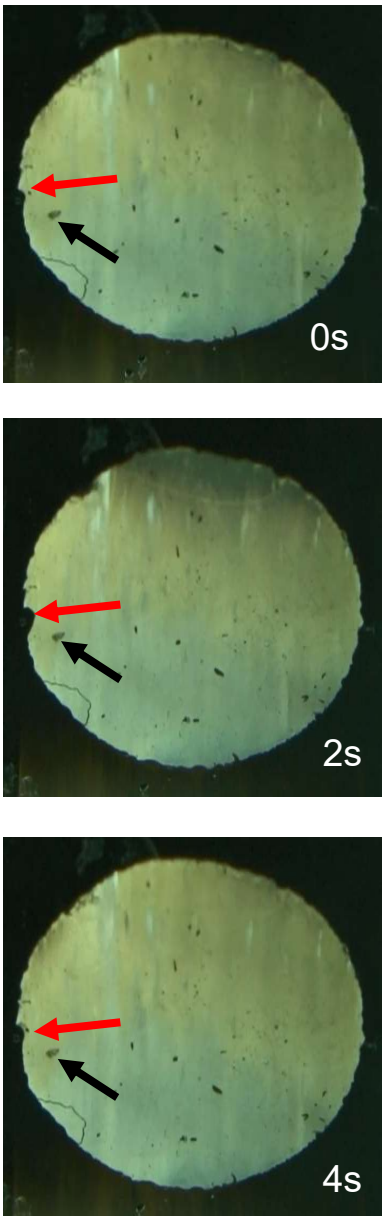

Figure 2-16. Time evolution of frictional interface in water, applied shear amplitude γ_{max} = 0.3 and angular frequency ω = 1 rad/s. An area pointed by a red arrow is a moving area and an area pointed by a black arrow is an area that do not move. White letters indicate the elapsed time from beginning of the observation.

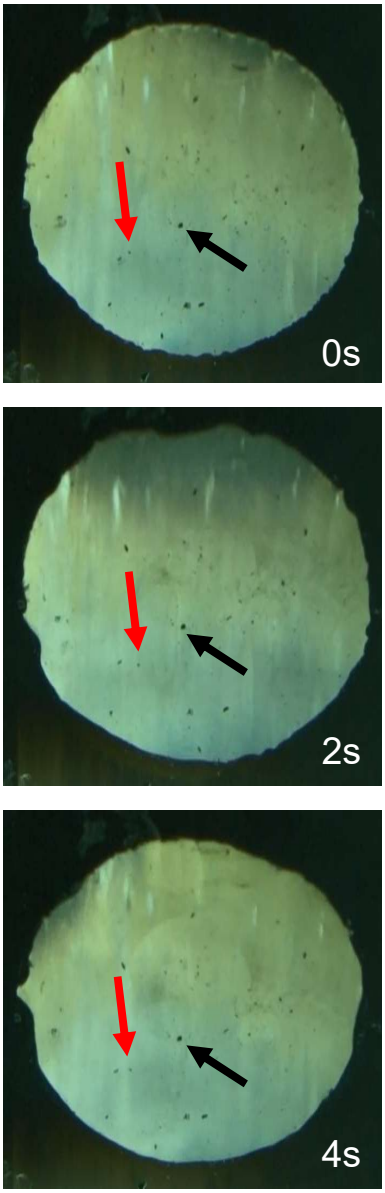

Figure 2-17. Time evolution of frictional interface in water, applied shear amplitude γ_{max} = 1.0 and angular frequency ω = 1 rad/s. An area pointed by a red arrow is a moving area and an area pointed by a black arrow is an area that do not move. White letters indicate the elapsed time from beginning of the observation.

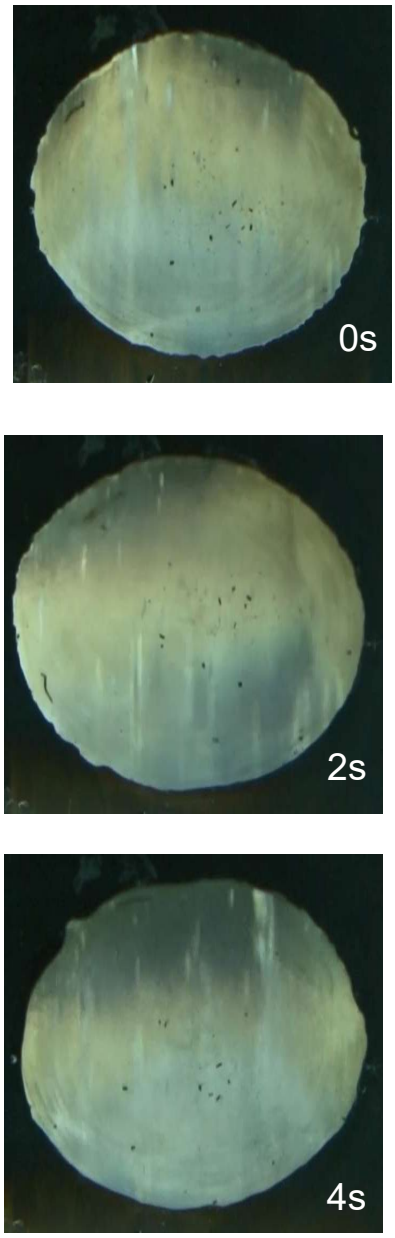

Figure 2-18. Time evolution of frictional interface in water, applied shear amplitude γ_{max} = 3.8 and angular frequency ω = 1 rad/s. Applied this strain amplitude, whole the frictional interface slid. White letters indicate the elapsed time from beginning of the observation.

Chapter 3. Non-Linear Analysis of Frictional Interface of Gel in Concentrated HA Solution

3.1 Introduction

In the previous chapter, I evaluated a transition from a linear to a non-linear response of oscillatory frictional test of gel in water. This analysis method is considered to be applicable to other systems. So, I adopted this method to gel friction in hyaluronic acid (HA) solution. HA is a polysaccharide contained in the synovial fluid of biological joints. Through this analysis, it may be possible to provide a way to elucidate the low friction of biological tissues.

3.2 Experiments

3.2.1. Materials

Hyaluronic acid (HA) (Mw = 1,900,000) was provided from Kikkoman Biochemifa Co. Schematic illustrations of HA is shown in Figure 3-1.

3.2.2 Hydrogels

Physically crosslinked PVA gels were used for this study. The method of gel preparation was described in chapter 2.

3.2.3. HA solution

The HA solution was used as a lubricant for the frictional test. Solution were prepared by mixing HA, water, and 0.1- M sodium chloride for an inhibition of HA aggregation and 0.2 g/L sodium azide for suppression of bacterial growth. The HA concentration of the

solution was 30c*, where c* was the overlapping concentration which is defined as the point where the concentration within a given conformation's pervaded volume is equal to the solution concentration[1]; that of this HA was 0.28 g/L calculated by a formula in Mendichi *et al*[2].

3.2.4. Viscosity measurement

The viscosity of concentrated HA solution was measured according to the procedure described in chapter 2.

3.2.5. Dynamic viscoelasticity measurement

The dynamic viscoelasticity of PVA gel was measured by ARES-G2 with parallel-plate (diameter: 25mm) at 25 ℃. Measurement method was the frequency sweep test in the angular frequency range ω of 0.1 ~100 rad s^{-1} at a shear strain of 0.5%.

3.2.6. Strain sweep test

The strain sweep test for gel friction in concentrated HA solution was performed according to the procedure described in chapter 2.

3.2.7. Oscillatory test for Lissajous curves

Oscillatory tests to obtain stress-strain Lissajous curves were performed to concentrated HA solution and the slidable gel in concentrated HA solution. The test procedure was described in chapter 2.

3.3 Results and Discussion

3.3.1. Rheological properties of concentrated HA solution

The HA solution shows typical rheological behaviors for concentrated polymer solutions, as shown in Figure 3-2. Figure 3-2(a) shows shear thinning in the high shear rate region, and Fig. 3-2(b) shows sol-gel transition at $\omega = 2$ rad/s.

3.3.2. Strain sweep test

Figure 3-3 is a graph superimposing the results of slidable gel in concentrated HA solution on Figure 2-10. For the friction of gel in concentrated HA solution, the slope of stress-strain curves was 1.0 in the small strain range as for the fixed gel and friction of gel in water. In water, the critical strain amplitude for the deviation from linearity occurred at quite a large value ($\gamma_{max,c} = 1$) and above this strain the stress started to decrease, while in concentrated HA solution, deviation from linearity occurred at a much smaller strain ($\gamma_{max,c} = 5 \times 10^{-3}$). Furthermore, the stresses at the large strain region ($\gamma_{max} = 2 \times 10^{-1}$) showed a peak in the HA solution, which differed from that in water. Furthermore, the stresses of the slidable gel in water were slightly lower than the fixed gel, almost independent of the normal pressure in the range of 11~44 kPa. On the other hand, in HA solution, the stresses were lower than those in water and increased as the normal pressure increased. These results indicate that HA solution forms a thin film at the gel/glass interface to reduce friction. A large normal pressure will squeeze out more of the HA solution to form a thinner film, therefore increasing the stress against the shear deformation. The deviation from the linearity suggests the slide of the gel under shear motion. Therefore, for the large strain range, $\gamma_{max} > \gamma_{max,c}$, the slidable gels should show a

non-linear viscoelastic response, and the maximum oscillatory shear stress, σ_{max}, estimated based on the assumption of a linear response, is no longer accurate.

3.3.3. Lissajous curves

Figure 3-4 and Figure 3-5 show the stress-strain Lissajous curves of HA solution and the slidable gel in HA solution, respectively. In Figure 3-4, the Lissajous curves showed good elliptical shapes, indicating that HA solution was linearly viscoelastic over the observed strain range. Figure 3-5 shows the Lissajous curves of slidable gel in HA solution. These Lissajous curves showed partially distorted elliptical shapes at very small strain γ_{max} = 0.001, even below the critical strain $\gamma_{max,c} = 5 \times 10^{-3}$ (Fig. 3-5[a]), and the distortion gradually increased with the strain until it reached a relatively large value (Fig. 3-5[b]). At a very large strain, the Lissajous curve also became a rectangular shape, indicating interfacial sliding, as also occurred in water. However, the sliding frictional stress in HA was one order of magnitude smaller than that in water. Such a friction reduction effect by HA solution at the interface is consistent with the result shown in Fig. 3-3.

3.3.4. Two dimensionless parameters for analysis of Lissajous curves

Figure 3-6 to 3-8 is graphs superimposing the results of slidable gel in concentrated HA solution on Figure 2-13 to 2-15, respectively. For HA solution, S values were almost zero, however κ values were around 0.6 (i.e., lower than 0.785), indicating that the HA solution is a linear viscoelastic system in the strain range observed. On the other hand, S and κ of the slidable gel in HA solution are very different from the behaviors of HA solution or slidable gel in water. The S of the slidable gel in the HA solution increased with γ_{max} even

from a very small strain (γ_{max} = 0.001), i.e., lower than the critical strain ($\gamma_{max,c}$ = 0.005), and reached very large values at large strains. On the other hand, κ increased gradually at $\gamma_{max} > \gamma_{max,c}$ and was across the red line (κ = 0.785) at around γ_{max} = 0.3 and saturated to κ = 0.9. This result indicates that for the slidable gels in the HA solution, both non-linearity and energy dissipation increase gradually with the strain, and the transition from a linear to a non-linear response is not as sharp as that for the slidable gel in water.

In HA solution, the HA film intercalated at the gel/glass interface screened the direct interaction of the PVA gel and substrate, which resulted in significant friction reduction. Accordingly, the non-linear viscoelastic behavior of the slidable gel in HA solution comes from the soft HA layer intercalated at the gel/glass interface. The rheology theory states that transient gel is formed when a concentrated polymer solution experiences a deformation with a strain rate faster than the inverse of the reptation time of the solution[1]. As shown in Figure 3-2(b), for the 30 c* HA solution used in this study, the angular frequency for the sol-gel transition was around 1 rad s^{-1}, above which the solution behaved like a transient gel with a dynamic modulus in the order of 100 Pa. Since the modulus of the transient gel is much softer than that of the PVA gel (54 kPa), the shear deformation is mostly exerted on the HA layer and the true strain of the HA layer is much larger than the nominal strain, γ_{max}, calculated from the thickness of the gel. Although the thickness of the HA layer is difficult to measure directly, a value in the range of 0.1~1 μm has been estimated from the frictional shear stress[3], which is 3-4 orders of magnitude lower than the bulk gel thickness (~1 mm) used to calculate the nominal strain γ_{max}. Accordingly, the true strain on the HA layer could be 3-4 orders of magnitude higher than the nominal value shown in Figure 3-3 and Figure 3-5. Accordingly, the strain rate exerted on the HA layer is 3-4 orders higher than the nominal strain rate, $\dot{\gamma} = \omega\gamma_{max}$.

Even for the minimum strain tested ($\gamma_{max} = 10^{-4}$) in this study, the true strain rate could be as high as 0.1~1 rad s^{-1}, which is close to the range of crossover angular frequency (G' = G'') for sol-gel transition (Fig. 3-2[b]). Such a high shear rate also induces shear thinning (Fig. 3-2[a]), and, therefore, the HA layer behaves as a transient physical gel to exhibit non-linear viscoelastic behavior even at a very small strain γ_{max}. Above the critical strain ($\gamma_{max,c} = 5 \times 10^{-3}$), the true strain becomes too high to rupture the transient gel. Therefore, the non-linear viscoelastic response of the slidable gel in HA solution is due to the dynamic rheological behaviors of the concentrated HA solution at the gel/glass interface.

3.4 Conclusion

From strain sweep tests, the slope of stress-strain curve at small strain region was 1, which indicated linear response, in any systems. However, the strain amplitude of deviation from linearity in concentrated HA solution was much smaller than that in water. Furthermore, the frictional stresses in HA solution were lower than that in water. It was suggested that frictional interface in HA solution was reduced friction due to remained HA solution. Furthermore, the thickness of residual HA solution at interface depended on the applied normal pressure, therefore, the frictional stress had a normal pressure dependence.

From analyses the Lissajous curves at each strain amplitude, it was found that the gel friction in HA solution was not caused by the simple friction between the gel and glass, but by the HA solution at the interface. Due to thin HA layer which behaves as a transient physical gel, the non-linear viscoelastic response of the slidable gel in HA solution exhibits the dynamic rheological behaviors of the concentrated HA solution at the gel/glass interface.

References

1 M. Rubinstein and R. H. Colby, “Polymer Physics.” Oxford University Press, Oxford. 2003.

2 R. Mendichi, L. Šoltés and A. G. Schieroni, “Evaluation of Radius of Gyration and Intrinsic Viscosity Molar Mass Dependence and Stiffness of Hyaluronan.” *Biomacromolecules*, **2003**, *4* (6), 1805-1810.

3 Y. Nakano, T. Kurokawa, M. Du, J. Liu, T. Tominaga, Y. Osada and J. P. Gong, “Effect of Hyaluronan Solution on Dynamic Friction of PVA gel Sliding on Weakly Adhesive glass Substrate.” *Macromolecules*, **2011,** *44*, 8908-8915.

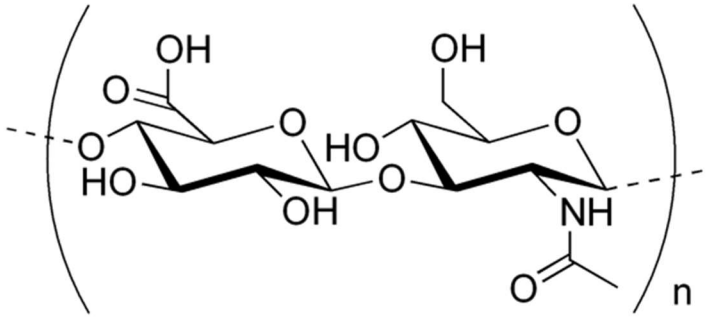

Figure 3-1. Chemical structure of HA.

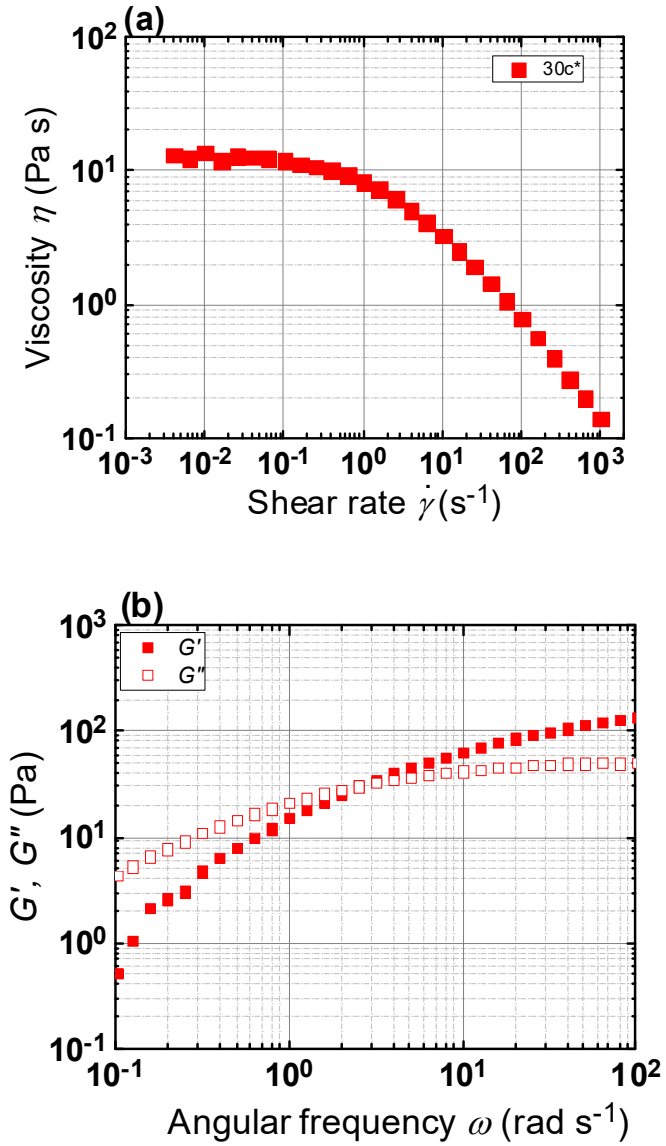

Figure 3-2. Rheological properties of concentrated HA solution at 25 °C. (a) shear rate dependence of viscosity η, (b) angular frequency dependence of storage modulus *G*' and loss modulus *G*" with shear strain of 0.5%. The crossover point between the *G*' curve and *G*" curve determines the inverse of the reptation time of the solution in (b). The molecular weight of HA = 1,900,000.

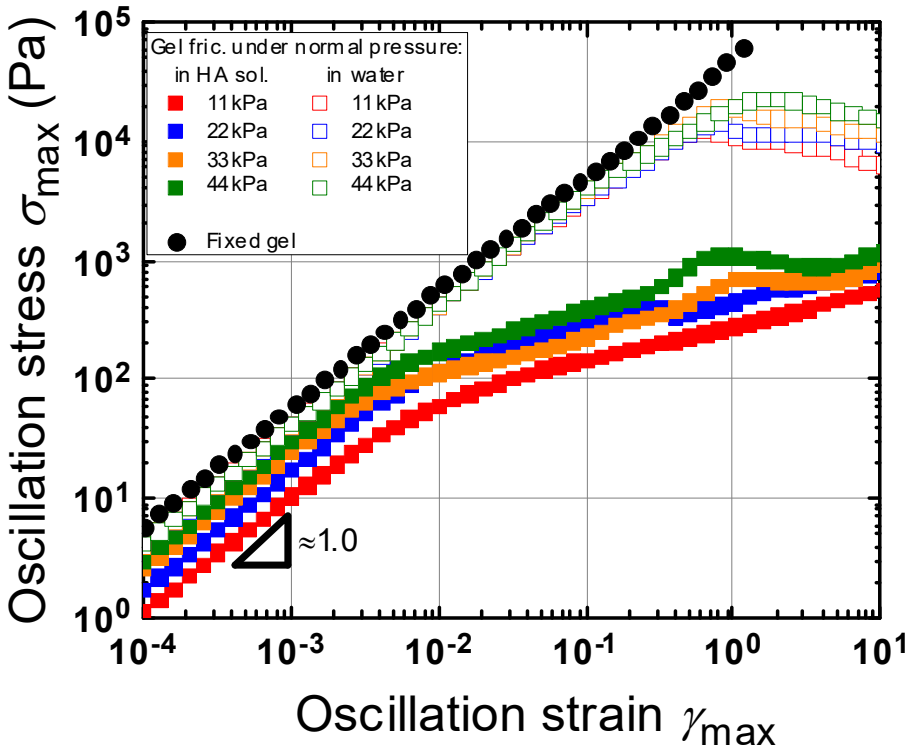

Figure 3-3. Strain sweep results of PVA hydrogel friction in liquid, measured by applying an oscillatory shear $\gamma_{max}\sin(\omega t)$ to slidable gel. The σ_{max} is the maximum oscillatory shear stress assuming a linear viscoelastic response of the system. The upper four curves show the results of oscillatory shear test in water, and lower four curves show those in 30 c* HA solution, under various normal pressures. Black closed circles show the strain sweep test of PVA gel bulk deformation using fixed PVA gel. Note that $\omega = 1$ rad s^{-1} was adopted.

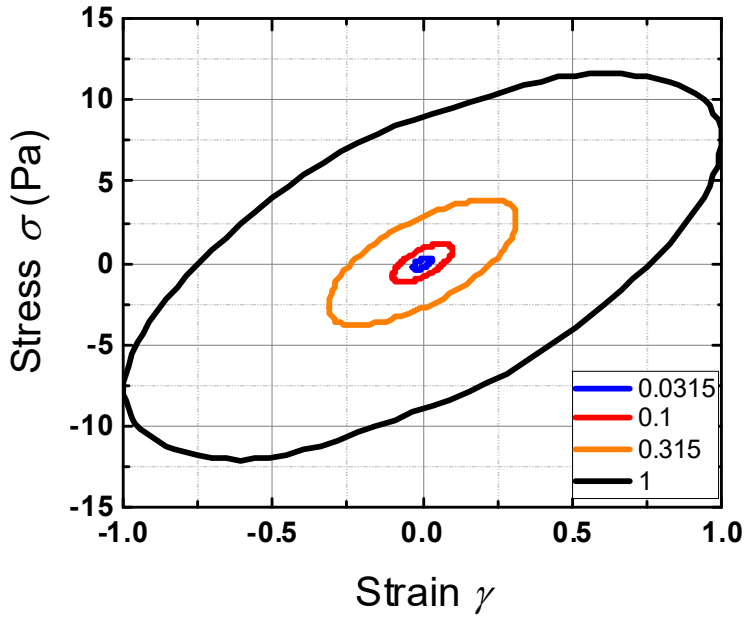

Figure 3-4. Lissajous curves of stress-strain of concentrated HA solution. The concentration of solution is 30 c*. The numbers in the figures are the applied strain amplitude γ_{max}. Applied angular frequency was $\omega = 1$ rad s^{-1}.

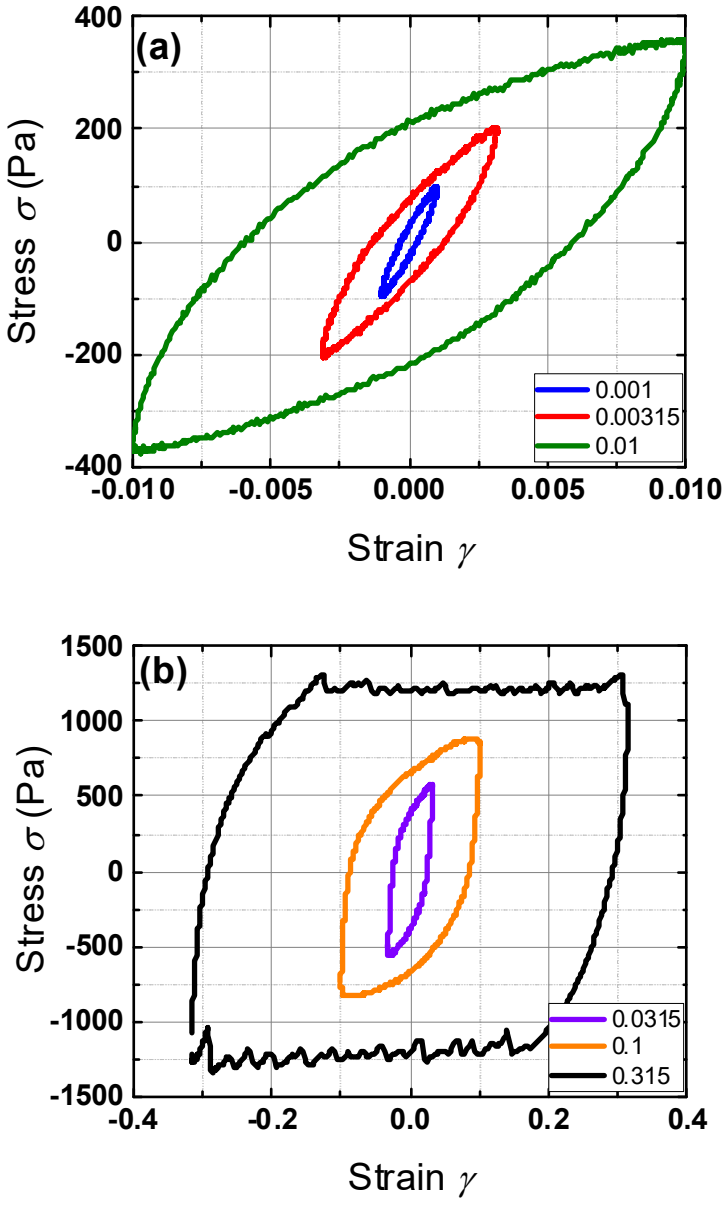

Figure 3-5. Lissajous curves of slidable gel in 30 c* HA solution at a normal pressure of 33 kPa. (a) small strain region (b) large strain region. The numbers in the figures are the applied strain amplitude γ_{max}. Applied angular frequency was $\omega = 1$ rad s^{-1}.

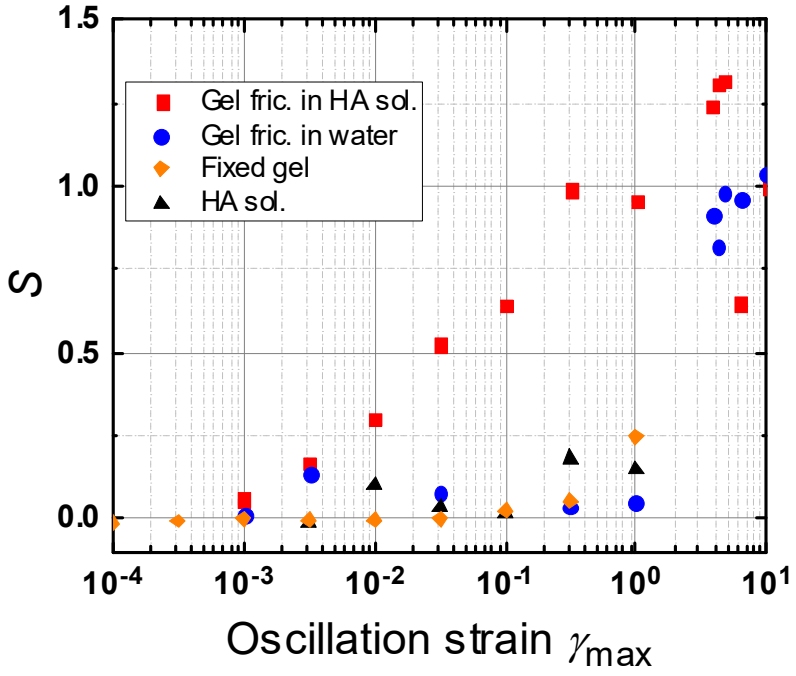

Figure 3-6. Oscillation strain dependence of S against applied maximum strain γ_{max} for various systems estimated from each Lissajous curves.

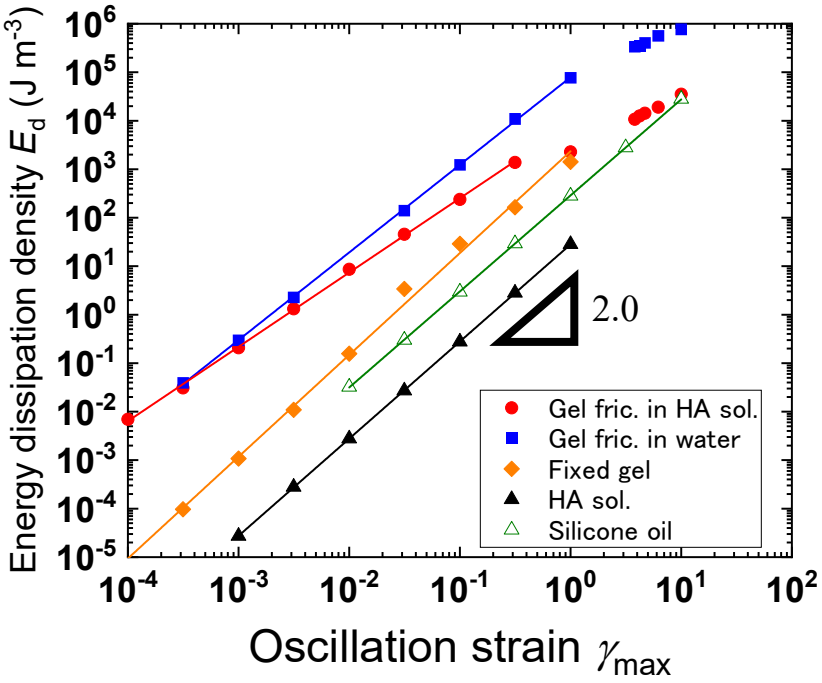

Figure 3-7. Oscillation strain dependence of an energy dissipation density E_d. E_d was estimated from 20th cycle Lissajous curves of each systems.

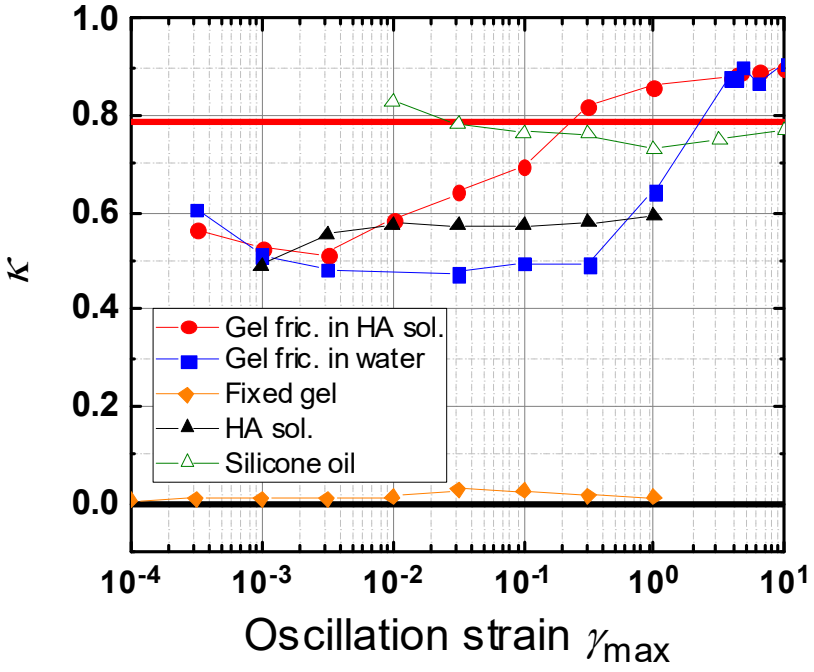

Figure 3-8. Oscillation strain dependence of occupancy parameter κ against applied strain amplitude γ_{max} for various systems estimated from each Lissajous curves. In this figure, the red line indicates κ = 0.785 for ideal viscous materials and the black line indicates κ = 0 for ideal elastic materials. The result of silicone oil is shown as a standard for the pure viscous liquid.

Chapter 4. Contact Pattern Formation by Oscillatory Shearing

4.1 Introduction

Soft matter has been extensively studied worldwide for its attractive properties. The development of new equipment and advances in analysis technique have also supported its research. However, many soft matter systems are non-equilibrium open systems, and it is reason why the research of soft matter complicates. Such complexity often appears in pattern in this world, for example, wind ripple, zebra stripes, coffee ring and so on[1]. In fact, the researches of pattern about soft matter are important topics[2-4]. Recently, our laboratory found contact pattern formation at frictional interface between gel and glass[5]. Patterns were observed various patterns by changing conditions, for example, concentration of hyaluronic acid (HA) solution, applied pressure to hydrogels, angular velocity and so on. All patterns were initially appeared at the periphery of disk-shaped gel, and spreaded to the center of gel. Here, I wondered; these patterns were observed in uni-directional rotational motion, how is the pattern observed in oscillatory motion? To clarify of this question, I observed the contact pattern in oscillatory motion. The results of the observation are expected to be a clue to clarify the principle of contact pattern formation.

4.2 Experiment

4.2.1 Hydrogels

Physically crosslinked PVA gels were used for this study. The method of gel preparation was described in chapter 2.

4.2.2 HA solution

Concentrated HA solutions were prepared for this study. The method of preparation of HA solution was same way in chapter 3.

4.2.3 *In situ* observation system for frictional interface

Gel/glass frictional interface in concentrated HA solution was observed according to the procedure described in chapter 2. In this chapter, I observed oscillatory frictional interface applied two γ_{max} = 1, 10 with ω = 1 rad/s. Furthermore, I also observed oscillatory frictional interface applied two ω = 0.1, 0.5 rad/s with γ_{max} = 10. Applied normal pressure is 33kPa.

4.3 Results and Discussion

4.3.1. *In situ* observation during oscillatory motion – effect of strain amplitude-

Figure 4-1 is a time evolution of oscillatory frictional interface. Applying strain amplitude γ_{max} was 1 and angular frequency ω was 1 rad/s. Dark image was observed at the beginning of oscillation. As time goes on, the contact area gradually increased from a periphery of disk-shaped gel. However, contact pattern was not observed 10 minutes later. On the other hand, Figure 4-2 shows a time evolution of oscillatory frictional interface applying strain amplitude γ_{max} = 10 and angular frequency ω = 1 rad/s. In this figure, the wavy pattern began to appear on the periphery of disk-shaped gel at 10 second after the beginning of oscillation. This pattern was not as clear as one applied uni-directional rotational motion, however, was still observed 10 minutes later. These results show the importance of strain amplitude to form contact pattern.

4.3.2. *In situ* observation during oscillatory motion – effect of angular frequency-

Next, the effect of angular frequency against contact pattern under constant strain amplitude was confirmed. Figure 4-3 and 4-4 show the time evolution of oscillatory frictional interface applying strain amplitude $\gamma_{max} = 10$, angular frequency $\omega = 0.5$ and 0.1 rad/s, respectively. Images were more indistinct than those of Fig. 4-2, however, patterns were observed in each image from 90 to 180 seconds. The interesting point was disappearing the patterns before 10 minutes later, differ to the observation applied $\omega = 1$ rad/s. These results suggest that the large strain amplitude is essential for an appearance of contact pattern, however, large angular frequency or high velocity is important for keeping of contact pattern.

4.4 Conclusion

Contact pattern formation at gel/glass interface was a phenomenon observed on not only uni-directional rotation motion but oscillatory motion. From this study, it was found that a strain amplitude threshold for contact pattern formation exists. Furthermore, it was suggested that not only strain amplitude but velocity was important for an contact pattern formation for long time.

References

1 M. C. Cross and P. C. Hohenberg, “Pattern formation outside of equilibrium.” *Rev. Mod. Phys.*, **1993**, *65* (3), 851-1112.

2 M. Kawaguchi, K. Shimomoto, A.Shibata and T. Kato, “Effect of anisotropy on viscous fingering patterns of polymer solutions in linear Hele-Shaw cells.” *Chaos*, **1999**, *9* (3), 323-328

3 J. Nase A. Lindner and C. Creton, “Pattern Formation during Deformation of a Confined Viscoelastic Layer: From a Viscous Liquid to a Soft Elastic Solid.” *Phys. Rev. Lett.*, **2008**, *101* (7), 074503.

4 C. S. Dutcher and S. J. Muller, “Effects of moderate elasticity on the stability of co- and counter- rotating Taylor-Couette flows.” *J. Rheo.*, **2013**, *57* (3), 791-812.

5 S. Yashima, S. Hirayama, T. Kurokawa, T. Salez, H. Takefuji, W. Hong and J. P. Gong, “Shearing-induced contact pattern formation in hydrogels sliding in polymer solution” *Soft Matter*, **2019**, *15*, 1953-1959.

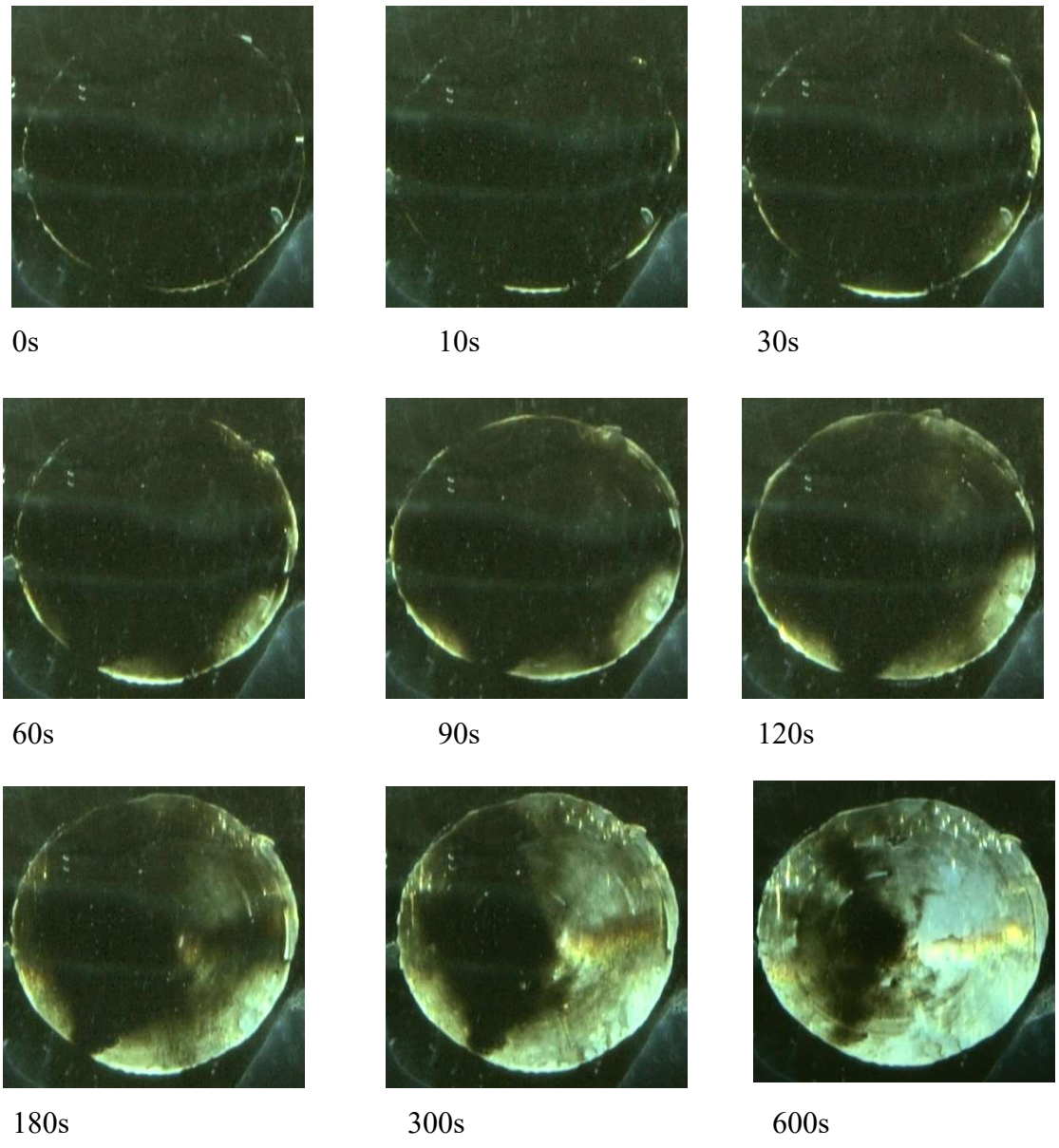

Figure 4-1. Time evolution of oscillatory frictional interface applied strain amplitude $\gamma_{max} = 1$, angular frequency $\omega = 1$ rad/s.

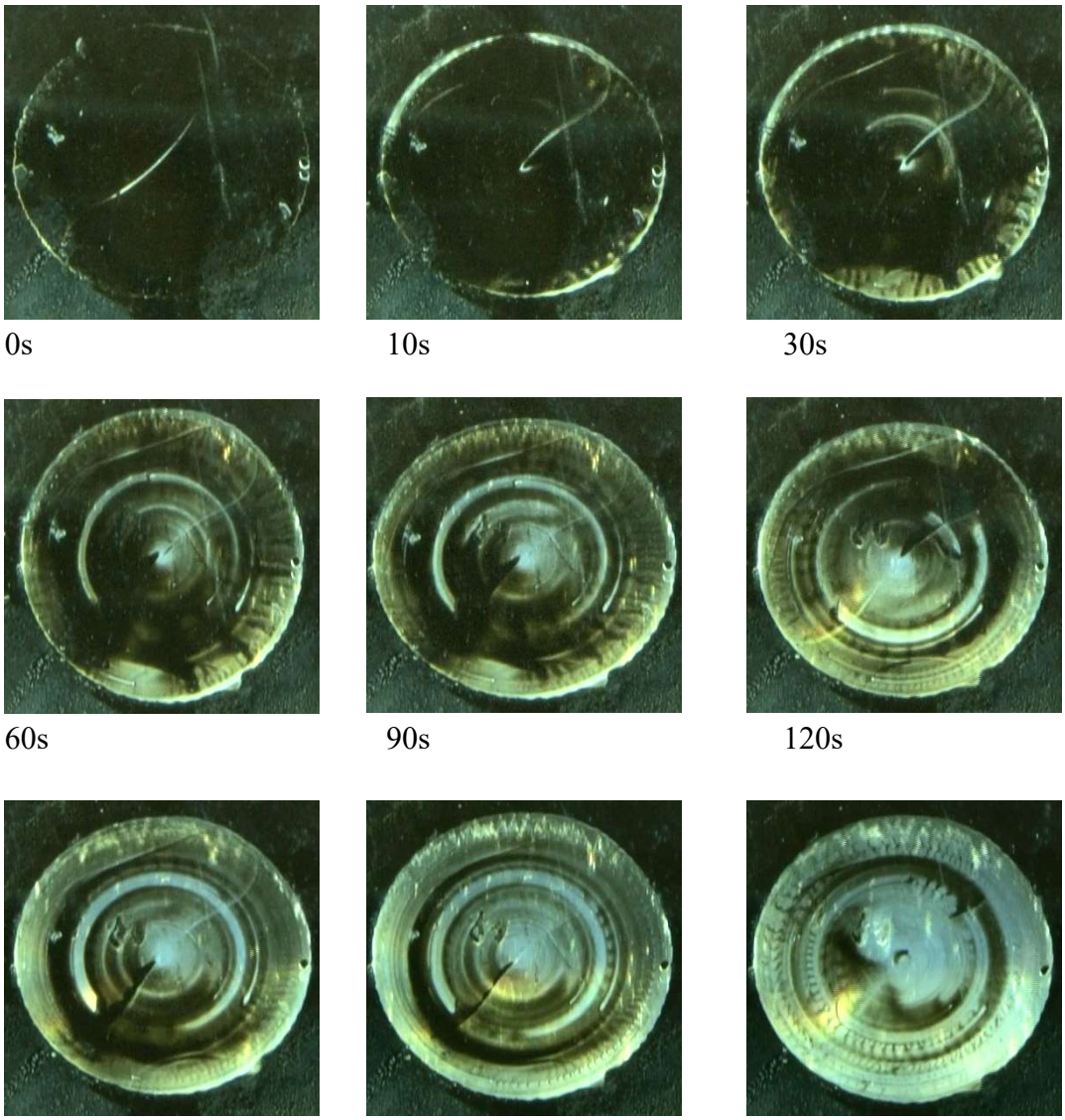

Figure 4-2. Time evolution of oscillatory frictional interface applied strain amplitude γ_{max} = 10, angular frequency ω = 1 rad/s.

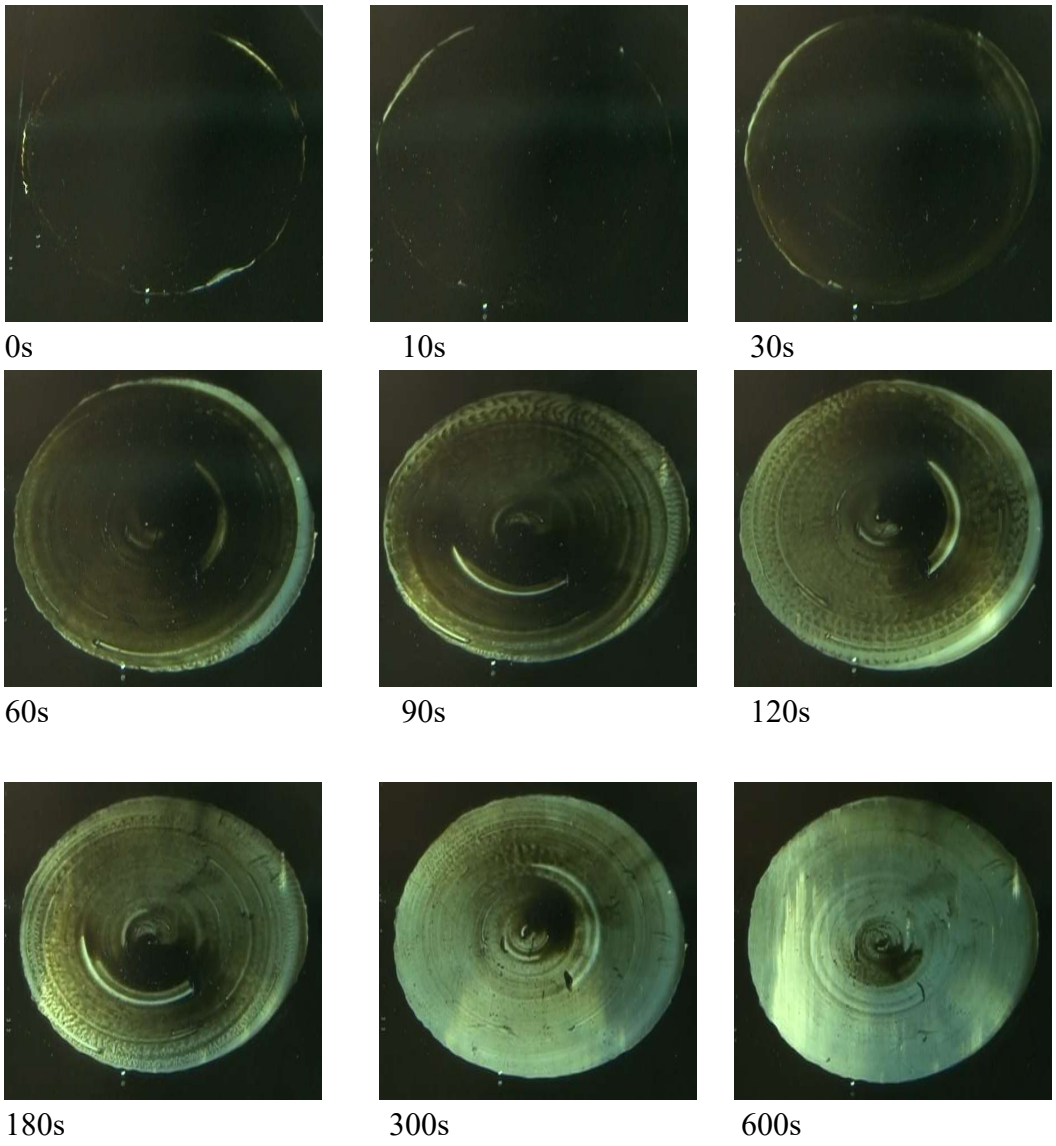

Figure 4-3. Time evolution of oscillatory frictional interface applied strain amplitude γ_{max} = 10, angular frequency ω = 0.5 rad/s.

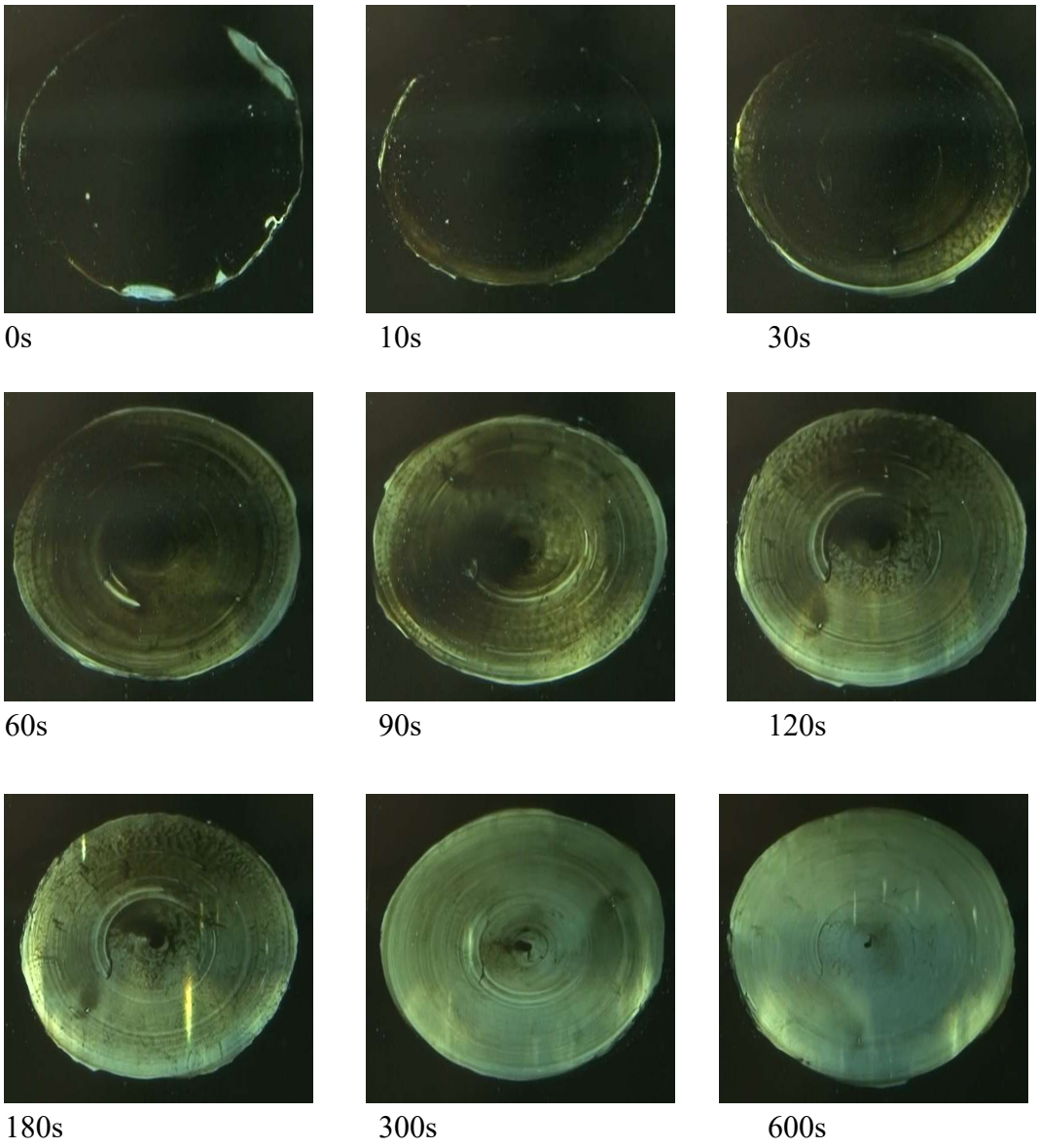

Figure 4-4. Time evolution of oscillatory frictional interface applied strain amplitude γ_{max} = 10, angular frequency ω = 0.1 rad/s.

Chapter 5. General Conclusion

In this study, I have analyzed gel friction using the results of oscillatory shear test.

In chapter 2, Oscillatory shear test and stress-strain Lissajous curves were useful approaches to characterize the non-linear viscoelastic behaviors and energy dissipation of hydrogel friction. By using two dimensionless parameters (the strain hardening ratio, S, and the energy dissipation occupancy, κ), the features of the Lissajous curves were well captured, which permitted us to systematically discuss the behaviors of the hydrogel friction in pure water with the increase of the strain amplitude γ_{max}. The slidable gel in water showed a clear transition from a linear viscoelastic response to a non-linear viscoelastic response at a critical strain amplitude $\gamma_{max,c}$, corresponding to the onset of macroscopic sliding. The energy dissipation at a small strain, even prior to the macroscopic sliding, indicated the dynamic effect of reversible bonds formed between the polymer chain and the substrate.

In chapter 3, I adopted the technique used in chapter 2 to the gel friction in concentrated HA solution. The slidable gel in HA solution showed remarkable friction reduction; however, the behavior is non-linear viscoelastic even at a very small γ_{max}, and the non-linearity and energy dissipation both gradually increase with γ_{max}. Such behavior is due to the non-linear rheological responses of the HA film intercalated at the gel/glass interface. The strain amplitude and strain rate exerted on the HA film were estimated to be 3-4 orders of magnitude higher than the nominal values to cause the non-linear viscoelastic response of the HA layer.

In chapter 4, contact pattern formation through oscillatory friction, I found a strain threshold of forming contact pattern. Strain amplitude is probably essential for

contact pattern formation. Furthermore, it was suggested the probability that the velocity at which strain applied was important for keeping contact pattern.

Finally, κ introduced in this study is a so convenient parameter that can be easily calculated regardless of the complexity of non-linearity. Thus, like $\tan\delta$ in dynamic viscoelastic measurements for linear responses, κ is a useful index to describe the viscoelastic properties of materials with non-linear responses.

List of publications

Original paper related to doctoral dissertation

S. Hirayama, T. Kurokawa and J. P. Gong, “Non-linear rheological study of hydrogel sliding friction in water and concentrated hyaluronan solution” *Tribology International*, **2020**, *147*, 106270.

Other paper

S. Yashima, S. Hiryama, T. Kurokawa, T. Salez, H. Takefuji, W. Hong and J. P. Gong, “Shearing-induced contact pattern formation in hydrogels sliding in polymer solution” *Soft Matter*, **2019**, *15*, 1953-1959.

Acknowledgement

This research on this dissertation has been carried out in the Laboratory of Soft and Wet Matter (LSW), Graduate School of Life Science, Hokkaido University, Japan, supervised by Professor Jian Ping Gong. Associate examiners are Professor Takayuki Kurokawa

Firstly, I express my appreciation to my supervisor, Professor Jian Ping Gong during my doctoral study in LSW. She gave me a chance to study in LSW, the fruitful discussion and suggestions about my research. I really respect her positive attitude, research understanding and considering.

Additionally, I would like to appreciate Professor Takayuki Kurokawa. I had less knowledge about gel friction when I joined LSW, but he told me basic knowledge about friction and how to use equipment, especially rheometer. Through the many discussion with him, I could get more knowledge and a milestone of this research.

I would like to many thanks also to Associate Professor Tasuku Nakajima, Assistant Professor Takayuki Nonoyama, Tenure Track Assistant Professor Daniel R. King and Assistant Professor Kunpeng Cui for their helpful scientific comments, many discussions and useful suggestions regarding my research. I am also very grateful to post-doctoral fellows, visiting researchers, research assistants and staffs in “LSW”.

Finally, special thanks to my parents for the support and during the life in Hokkaido University.

Satoshi Hirayama

June 2020